

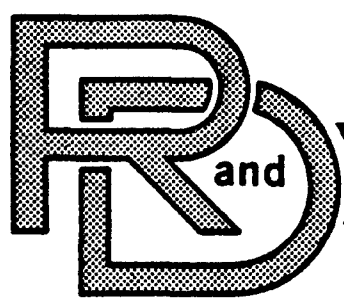
2016

990

A157667

Reproduced From
Best Available Copy

A0A157667



CENTER
LABORATORY
TECHNICAL REPORT

NO. 13099



The Recycling and Reclamation of Used Tank Track Pins

J.F. Wallace & J.T. Snyder
Case Western Reserve University
Department of Metallurgy & Mat'l Sci.
10900 Euclid Avenue
Cleveland, Ohio 44106

by

Approved for Public Release:
Distribution Unlimited

20020726104

U.S. ARMY TANK-AUTOMOTIVE COMMAND
RESEARCH AND DEVELOPMENT CENTER
Warren, Michigan 48090

AN-46863

REPORT DOCUMENTATION PAGE

Unclassified

1a. REPORT SECURITY CLASSIFICATION		1b. RESTRICTIVE MARKINGS	
2a. SECURITY CLASSIFICATION AUTHORITY		3. DISTRIBUTION/AVAILABILITY OF REPORT	
2b. DECLASSIFICATION/DOWNGRADING SCHEDULE		Approved for public release; distribution unlimited	
4. PERFORMING ORGANIZATION REPORT NUMBER(S)		5. MONITORING ORGANIZATION REPORT NUMBER(S)	
13099			
6a. NAME OF PERFORMING ORGANIZATION	6b. OFFICE SYMBOL (if applicable)	7a. NAME OF MONITORING ORGANIZATION	
Case Western Reserve Uni.		U. S. Army Tank Automotive Command	
6c. ADDRESS (City, State, and ZIP Code)		7b. ADDRESS (City, State, and ZIP Code)	
10900 Euclid Avenue Cleveland, Ohio 44106		Warren, MI 48397-5000	
8a. NAME OF FUNDING/SPONSORING ORGANIZATION	8b. OFFICE SYMBOL (if applicable)	9. PROCUREMENT INSTRUMENT IDENTIFICATION NUMBER	
Joe Fix	AMSTA-RCKT	DAAE07-83-K-R004	
8c. ADDRESS (City, State, and ZIP Code)		10. SOURCE OF FUNDING NUMBERS	
Warren, MI 48397-5000		PROGRAM ELEMENT NO.	PROJECT NO.
		TASK NO.	WORK UNIT ACCESSION NO.
11. TITLE (Include Security Classification)			
"The Recycling and Reclamation of Used Tank Track Pins"			
12. PERSONAL AUTHOR(S)			
Joseph T. Snyder and John F. Wallace			
13a. TYPE OF REPORT	13b. TIME COVERED	14. DATE OF REPORT (Year, Month, Day)	15. PAGE COUNT
Final Technical	FROM Mar '83' TO Aug '85	August 1985	62
16. SUPPLEMENTARY NOTATION			
17. COSATI CODES			18. SUBJECT TERMS (Continue on reverse if necessary and identify by block number)
FIELD	GROUP	SUB-GROUP	
19. ABSTRACT (Continue on reverse if necessary and identify by block number)			
<p>This investigation was directed at determining the feasibility of recycling used tank track pins. Tank track pins manufactured from SAE 8650H alloy steel bar were tested in bending fatigue thus establishing the fatigue life characteristics of production pins. These pins were quenched and tempered, induction hardened and shot peened during manufacturing. To determine recycleability, several pins were fatigued at various stress levels to approximately 80 percent of their expected life, and reprocessed to the original specifications. After checking for cracks, these pins along with others which received only the reheat treatment, were fatigued to failure. Microhardness, metallographic and surface residual stress measurements were conducted at various stages of testing and reprocessing to observe changes that may occur.</p>			
20. DISTRIBUTION/AVAILABILITY OF ABSTRACT		21. ABSTRACT SECURITY CLASSIFICATION	
<input checked="" type="checkbox"/> UNCLASSIFIED/UNLIMITED <input type="checkbox"/> SAME AS RPT. <input type="checkbox"/> DTIC USERS		Unclassified	
22a. NAME OF RESPONSIBLE INDIVIDUAL	22b. TELEPHONE (Include Area Code)	22c. OFFICE SYMBOL	
John F. Wallace	(216) 368-4222	Met. & Mat'l Sci.	

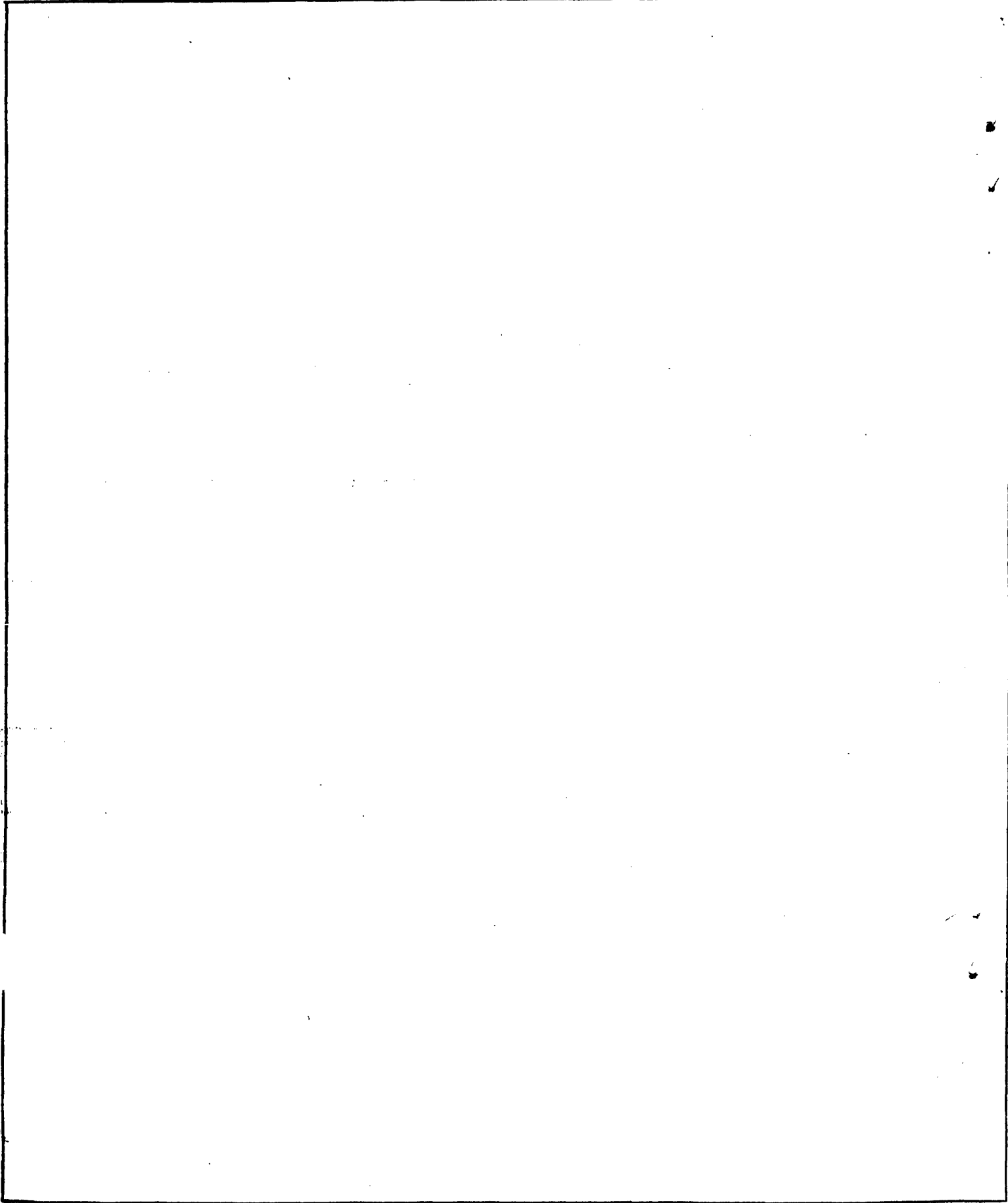


TABLE OF CONTENTS

Section	Page
1.0. INTRODUCTION	9
2.0. OBJECTIVE	9
3.0. CONCLUSION	10
4.0. RECOMMENDATIONS	10
5.0. DISCUSSION	11
5.1. <u>General</u>	
5.1.1 <u>Literature Review</u>	11
5.1.2. <u>Fatigue Behavior</u>	11
5.1.3. <u>Nucleation of Fatigue Cracks</u>	13
5.1.4. <u>Removal of Fatigue Damage by Treatment</u>	13
5.2. MATERIAL AND PROCEDURE	15
5.2.1. <u>Materials</u>	15
5.2.2. <u>Reprocessing of Pins</u>	18
5.2.3. <u>Fatigue Testing</u>	18
5.2.4. <u>Microhardness Testing</u>	21
5.2.5. <u>Metallographic Testing</u>	21
5.2.6. <u>Nondestructive Testing of Tank Track Pins</u>	21
5.2.7. <u>Statistical Analysis of the Fatigue Data</u>	22
5.2.8. <u>Residual Stress Measurement</u>	23
5.3. RESULTS AND DISCUSSION	23
5.3.1. <u>Fatigue Test Results</u>	23
5.3.1.1. <u>As Received Pins</u>	23
5.3.1.2. <u>Reheat Treated Pins</u>	37
5.3.1.3. <u>Recycled Pins</u>	37
5.3.2. <u>Microhardness Test Results</u>	41
5.3.2.1. <u>As Received Pins</u>	41
5.3.2.2. <u>Fatigued Pins</u>	41
5.3.2.3. <u>Reheat Treated Pins</u>	41
5.3.3. <u>Metallographic Results</u>	48
5.3.3.1. <u>As Received Pins</u>	48
5.3.3.2. <u>Fatigued Microstructure</u>	48
5.3.3.3. <u>Reheat Treated Pins</u>	48
5.3.4. <u>Surface Residual Stress Results</u>	48
5.3.4.1. <u>As Received Pins</u>	48
5.3.4.2. <u>Reheat Treated Pins</u>	56
5.3.5. <u>Nondestructive Testing of Pins</u>	56

TABLE OF CONTENTS (Continued)

LIST OF REFERENCES 59

DISTRIBUTION LIST DIST-1

LIST OF ILLUSTRATIONS

Figure	Title	Page
5-1.	An Idealized Fatigue or S-N Curve for a Steel Sample	12
5-2.	A Schematic Drawing of a Cross Sectional View of Slip Bands at the Surface of a Fatigued Material	14
5-3.	A Reproduction of Drawing No. 11645132 Showing Tank Track Pins T-142	16
5-4.	The Fixturing of the MTS used to Fatigue Test Tank Track Pins in Four Point Bending	19
5-5.	A Plot of the Data and the S-N Curve of Tank Track Pin T-142 As Received	27
5-6.	A Plot of the Statistical S-N Curves of the As Received Tank Pins	28
5-7.	A Plot of the Data and the S-N Curve of Tank Track Pin T-142 after Reheat Treatment	29
5-8.	The S-N Curve of as Received and Reheat Treated Tank Track Pin T-142	30
5-9.	The Plot of the Statistical Median Rank of Fatigue Data on As Received Pin at Different Stress Levels	33
5-10.	An Unetched Micrograph of the Surface of an As Received Pin after 23,851 Cycles	35
5-11.	A Fracture Surface of an As Received Tank Track Pin	36
5-12.	A Typical Fracture Surface of a Fatigued Pin that had Undergone Reheat Treatment	40
5-13.	A Micrograph Showing the Cross Section of the Crack Origin of Recycled Pin that Failed Prematurely	42
5-14.	Hardness Traverse from the O.D. to the I.D. of Tank Track Pin T-142 As Received	43
5-15.	Hardness Traverse from the O.D. to the I.D. of Tank Track Pin T-142 after Fatigue Cycling	44

LIST OF ILLUSTRATIONS (Continued)

Figure	Title	Page
5-16.	Hardness Traverse from the O.D. to the I.D. of Tank Track Pin T-142 after being Fatigued to Failure	45
5-17.	Hardness Traverse from the O.D. to the I.D. of Tank Track Pin T-142 after Reheat Treatment	46
5-18.	Hardness Traverse from the O.D. to the I.D. of Tank Track Pin T-142 which was Subjected to Fatigue Stressing	47
5-19.	The Microstructure of an As Received Pin Showing the Induction Hardened Zone	49
5-20.	The Core Microstructure of an As Received Pin Showing Coarse Tempered Martensite	50
5-21.	A Micrograph Showing the Transition Zone between Figures 7.3.1.a and b	51
5-22.	A Micrograph of the Surface of a Fatigued, but not Failed Tank Track Pin	52
5-23.	A Micrograph of a Recycled Tank Track Pin Showing the Surface Microstructure	54
5-24.	A Photo of a Tank Track Pin that was Fatigued until a "Ping" Indicated the Presence of a Crack	55
5-25.	A Fractograph of a Recycled Pin that Failed Prematurely after Reheat Treatment when Testing was Continued	57

LIST OF TABLES

Table	Title	Page
5-1.	Nominal Composition Ranges of AISI-SAE 8650H Alloy Steel	17
5-2.	Results of Bending Fatigue Tests Conducted On As Received, T-142 Tank Track Pins	24
5-3.	Results of Bending Fatigue Tests Conducted on Reheat Treated Tank Track Pins	25
5-4.	Results of Bending Fatigue Tests Conducted on Fatigued and Reheat Treated Tank Track Pins	26
5-5.	Results of Microhardness Traverses through Tank Track Pins from Surface to I.D. at Various Stages of Testing	31
5-6.	The Statistical Evaluation of the As Received Pin Fatigue Data using the Rank Method	38
5-7.	Results of Residual Stress Measurements of Tank Track Pins in Various Conditions	53

THIS PAGE LEFT BLANK INTENTIONALLY

1.0. INTRODUCTION

This investigation was directed towards determining the feasibility of reheat treating used tank track pins so that they can be used as replacement pins on tank tracks. The primary emphasis was placed on the study of tank track pin T-142 (Part Number 11645132). This pin is representative of a number of similar track pins that are produced from the same material and processing, but have different dimensions. The results from this investigation can be applied to these other pins. A tank track pin is a vital component in the track assembly of U.S. Army tanks. A total of 180 pins in rubber bushings are linked together in track shoes to comprise one tank track. These pins are presently subject to failures in service, mostly from fatigue. The fatigue failures are the result of the high loads from the weight of the tank, which are concentrated into high bending stresses in the pin by the track shoe which holds the pin.

2.0. OBJECTIVE

Because of the failure problems, considerable work has been expended in materials selection and in processing to enhance the fatigue performance of the pins. The material used to fabricate the pins is Society of Automotive Engineers 8650H alloy steel. The pins are quenched and tempered to a uniform hardness of 40 to 45 Rockwell C followed by induction hardening to Rockwell C 55 to 60 to a minimum depth of 0.060 inch. By properly heat treating and induction hardening this material, compressive residual stresses are induced into the surface, thus improving the fatigue strength. By using a final shot peening process, additional residual stresses are increased to approximately one half the yield strength, further improving the fatigue strength. Even with the use of all these methods of improving the fatigue properties, pin failures are still significant.

The current solution to the problem of pin failures is to replace the pins during the normal maintenance of the tank. During this maintenance the track is removed from the tank and disassembled. The pins are then removed from the track shoe and discarded because the amount of damage in any pin is unknown. This discarding of pins represents a cost in material and processing of the pins. Since not all pins have been permanently damaged during service use, if a way to recycle the pin were established, this would produce a net savings in time and materials. This investigation proposed to examine the feasibility of recycling the used tank track pins removed during track maintenance. The recycling procedure is designed to reprocess the pins to the original specifications, thus removing any damage that has occurred. The success of this project is based on the ability of the reheat treatment to eliminate the damage caused by high dynamic loading.

To test the recycleability of the pins, fatigue testing was used to determine the fatigue curve of the tank pins in the new or as received condi-

tion. Pins were then fatigued to a known portion of their fatigue life and then recycled using the original heat treatment to remove any fatigue damage which had not developed into a microcrack. After recycling, fatigue testing was conducted to determine whether the fatigue life of the pins had been recovered.

3.0. CONCLUSIONS

The reheat treatment of the tank track pins can accomplish a restoration of nearly all the original fatigue strength in pins fatigued to about 80 percent of the number of cycles to failure. If the pins are cracked on their outer surface by previous fatigue stresses or quench cracking during reheat treatment, the fatigue life is very poor. Since the surface of the pin is under residual compressive stress after the processing, the detection of these fine cracks is difficult and best undertaken before shot peening.

The microhardness readings across the section of the pins in various conditions including as received or new, reheat treated, fatigued and reheat treated (recycled), and after fatigue testing do not indicate any effect of fatigue stressing.

The microstructure of the pins fatigued to failure showed the presence of slip bands along the maximum shear stress plane in the highly stressed surface. These bands are removed by reheat treatment.

Residual stress measurements made on the pins in various conditions show how processing and stressing of the pins influence the compressive surface stresses. After induction hardening, the surface stresses were -15 ksi; this increased to -110 ksi after the pins were processed completely through shot peening. After fracture from fatigue stressing, the surface stress was reduced to as low as -32 ksi at the fatigue crack, although it was -90 ksi at a 0.25 inch from the crack. The reheat treated and reshot peened pins tested only had -90 ksi residual stress after shot peening, apparently because smaller size shot was employed.

4.0. RECOMMENDATIONS

It is recommended that a pilot lot of tank track pins that have been removed in the used but uncracked condition during the overhaul of tank tracks be recycled as described in this report. The performance of this pilot lot of recycled pins can then be compared to new pins. Acceptable behavior of recycled pins would indicate that the general recycling of used, but uncracked, tank track pins should be considered.

5.0. DISCUSSION

5.1. General

5.1.1 Literature Review

5.1.2. Fatigue Behavior. Fatigue by definition, is the weakening, or failure of a material because of dynamic loading at stress levels that are safe under static conditions¹. The general, characteristics of the fatigue response of a material are recorded using a fatigue or S-N curve, which plots the lifetime in cycles as a function of the alternating maximum stresses². This curve is plotted on semi-log or log-log coordinates. An idealized fatigue curve is shown in Figure 5-1 with two regions of interest. The first is the finite life period at higher stresses where the lifetime increases with decreasing stress. The second region is below a stress called the endurance limit where the tested material has an infinite life.

The fatigue process has been studied in depth by many authors. The general observations show that slip band formation, fatigue hardening or softening, crack nucleation, crack growth along the maximum shear stress plane, crack growth normal to the maximum principal stress, and then the final failure in one or a few stress cycles are the various stages of the fatigue process²⁻⁹. The proportion of the life that is associated with each of these stages, however, cannot be completely generalized. The relative length of each stage is dependent on the material, the condition of the material, geometry of the part, and testing conditions^{5,10,11}. The stress level of the endurance limit also depends on many variables which include the type of material, the tensile strength, grain size, notch sensitivity, surface finish, part design (geometric stress raisers), surface residual stress state, type of loading, and environment^{3,11,12}. With all these considerations, fatigue becomes one of the more complicated aspects of design for normal usage. The problem of fatigue is enhanced when safety factors are required to be small due to considerations such as weight reduction. In aerospace, hydrospace, aircraft, and military applications design for weight savings has pushed the need for improved fatigue performance without the increase in dimensions.

Methods to improve the fatigue performance in steels include raising the tensile strength of the material at the surface with such methods as carburization, nitriding, flame hardening, induction hardening, and other surface treatments³. Other improvement methods center around improving the surface condition and the residual stress state of the surface. In one investigation, improvements of over a 100 percent increase in fatigue life have been reported by polishing lathe-formed specimens¹³. In other investigations, compressive residual stresses in the surface have been shown to greatly improve the fatigue properties of most materials^{14,15}. The methods to create compressive surface residual stresses include quenching low hardenability steels, induction hardening, shot peening, and surface rolling¹⁵.

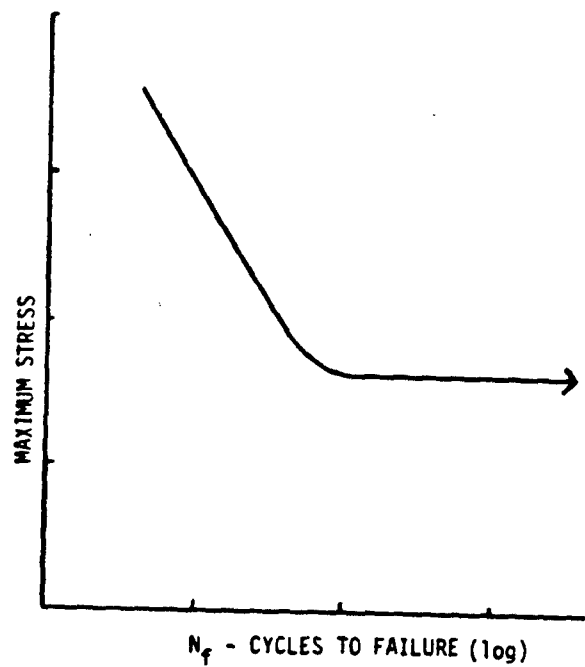


Figure 5-1. An Idealized Fatigue or S-N Curve for a Steel Sample.

5.1.3. Nucleation of Fatigue Cracks. Many discussions have been written concerning the cause of fatigue failures. It has been shown that fatigue cracks are generated from slip bands¹⁶. Slip bands are believed to be formed by the movement of dislocations, that are generated near the surface, along active slip systems which parallel the maximum shear stress direction¹⁶. The movement of these dislocations is not reversible during the stress reversal of the fatigue cycle. This is microplastic slip, and is the damage that accumulates to cause final failure. Slip bands are exposed at a free surface and result in the displacement of layers of material called intrusions and extrusions^{17,18}. Figure 5-2 illustrates an idealized cross section of a slip band showing these intrusion and extrusions and how they are believed to develop into cracks⁸. The general models of fatigue crack nucleation have been grouped into five main categories which are:

- models which consider the growth of microcracks as the continuation of deepening slip band intrusions which form early in the fatigue life;
- models that hypothesize microcracks are the result of localized brittle fracture of the material;
- models that have vacancy coalescence as the source of fatigue microcracks;
- dislocation models that show crack formation as the accumulation of defects and subsequent loss of coherency across a slip plane; and,
- models based on nucleation of cracks from grain boundaries^{4,7,17}.

Whatever the mechanism or combination of mechanisms are, fatigue will occur in a vacuum or any other atmosphere, as well as at low temperatures (4.5°K) or high temperatures (at high temperatures with creep)^{16,17}. Fatigue crack nucleation has been shown to be always associated with the surface or an interface in the sample. In addition to this, investigations have shown fatigue damage to be limited to the surface of the sample when no other interface is present¹⁶. In these experiments, the surface of fatigued samples tested in repeated tension was removed at regular intervals during the expected lifetime of the sample. When the same stress level was used throughout the test, the life of the specimen was only limited by the amount of material. Other experiments show that the fatigue life of a sample cut from the inside of a larger axially fatigued sample has the same fatigue life as a nonfatigued sample¹⁹. Oxygen has also been shown to play an important role in the formation of fatigue cracks, but this role is not vital since fatigue will occur at higher stresses in a vacuum²⁰.

5.1.4. Removal of Fatigue Damage by Treatment. Several authors have considered the question of whether or not fatigue damage can be removed from a

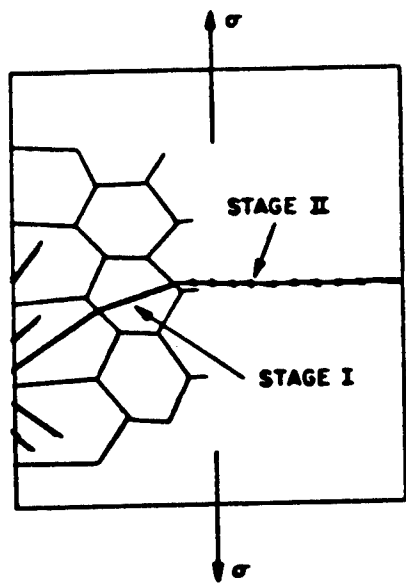


Figure 5-2. A Schematic Drawing of a Cross Sectional View of Slip Bands at the Surface of a Fatigued Machine.

material by a suitable heat treatment. Two distinct ideas on this subject with considerable difference in opinion have been presented. The first contends that fatigue is in many ways like cold work since both are associated with the plastic flow of the material, differing only in magnitude. Structural changes that occur during cold work can be annealed out and the material then cold worked further^{3,21}. Likewise fatigue damage, which consists of microplastic strain, can be removed by a suitable heat treatment, if the treatment is conducted before a microcrack is formed. The other point of view disagrees with this; it is maintained that permanent fatigue damage is developed very early in the fatigue life, possibly during the first stress cycle^{19,22,23,24}. Experimental evidence seems to indicate that the latter is true. But the same evidence does not disprove the first view either. Experiments have been conducted on nickel, brass, aluminum, copper, silver, gold, and iron but not in steel^{23,25,26}. These experiments were generally conducted by interrupting fatigue tests at regular intervals and annealing the tested samples. Intermediate anneals were generally given at every 20 percent or 50 percent of the expected life of the sample. These tests showed that no significant difference existed between the total life of these samples and of those that received no intermediate anneal. The conclusion from one of these tests was that surface notching from slip bands is the factor responsible for the lack of recovery of the fatigue properties²⁵.

5.2. MATERIAL AND PROCEDURE

5.2.1. Materials

The major focus of this investigation involved the testing of tank track pin T-142. The processing and materials used in the production of this pin are specified in Drawing No. 11645132 which is shown in Figure 5-3. The pins are produced from 8650H alloy steel bar, the nominal composition ranges for which are listed in Table 5-1. The pins are machined to about a 1.25-inch diameter, 28-inch length with a 0.5-inch central hole drilled the entire length. The O.D. of the pin has a 63-microinch finish and the I.D. a 125-microinch finish. One 1.81-inch long flat with a maximum depth of 0.169-inch is machined starting at 0.31-inch from either end. After machining, the pin is austenitized, quenched, and tempered to a Rockwell C (Rc) hardness of 40 to 45, then induction hardened on the surface to Rc 55 to 60, to a depth of 0.060-inch minimum. No more than 0.005-inch partial decarburization is permitted. The final operation, after straightening if needed, is shot peening to about 0.012C-Almen strip intensity with 390 or 460 steel shot. These pins were manufactured at, and received from, the Blairsville Machine Company of Blairsville, Pennsylvania.

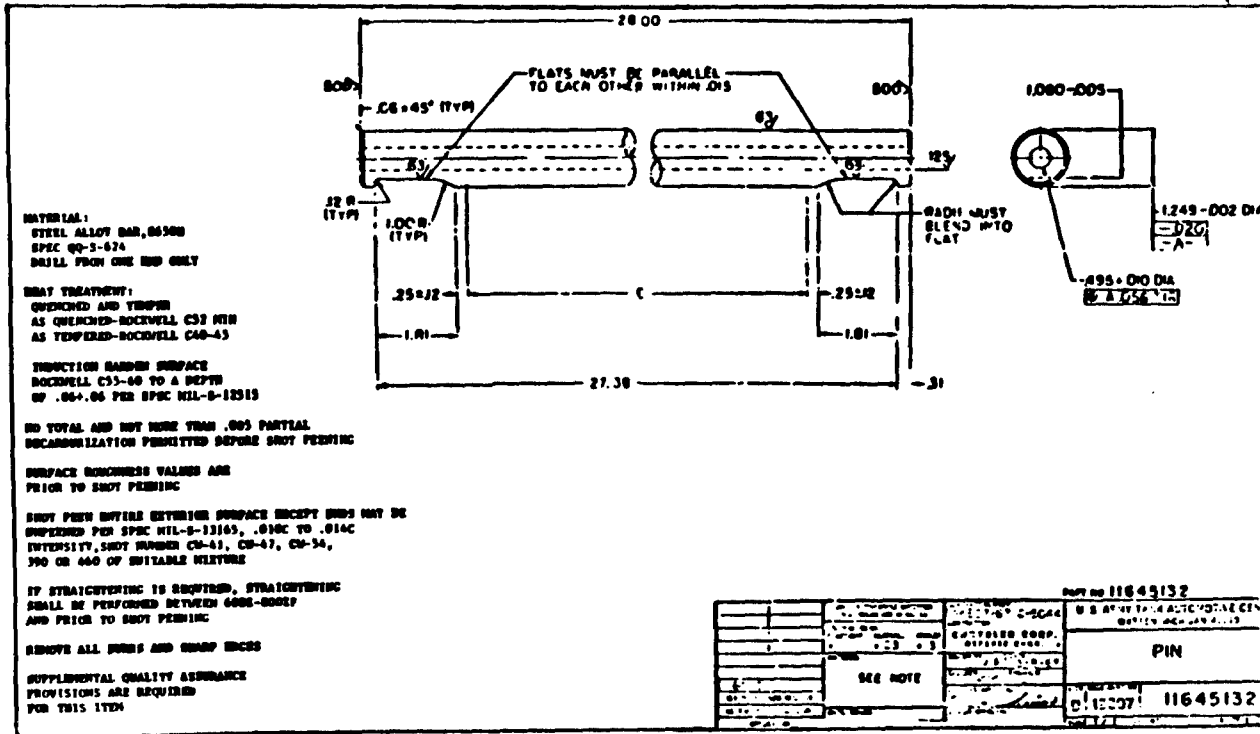


Figure 5-3. A Reproduction of Drawing No. 11645132 Showing Tank Track Pin T-142.

Table 5-1. Nominal Composition Ranges of AISI-SAE 8650H Alloy Steel.

Carbon	0.47% to 0.54%
Manganese	0.70% to 1.05%
Nickel	0.35% to 0.75%
Chrome	0.35% to 0.65%
Molybdenum	0.15% to 0.25%

Metals Handbook, 9th Edition, Vol. 1, ASM, Metals Park, Ohio 1978, pp. 125-130.

5.2.2. Reprocessing of Pins

The reheat treatment used in the recycling of pins was designed to duplicate the original processing. Two sets of pins were sent to commercial sources for reprocessing. The first set, which consisted of four pins that were as received, was reprocessed to determine the effect of the reheat treatment on nonfatigued pins. These pins will be referred to as the reheat treated pins. The second set includes pins that were fatigued at CWRU at various stress levels, to a number of cycles that was just short of failure (80 percent to 90 percent of expected life). These pins will be referred to as the recycled pins. The first stage of heat treatment was conducted at Horsburgh & Scott Co. of Cleveland, Ohio. This heat treatment began with an austenization at 1575°F in a carbon controlled gas furnace, followed by an oil quench and temper. The temper treatment was conducted at 700°F, producing a hardness of Rc 45. The next stage of reheat treatment was induction hardening performed at Euclid Heat Treating Co. of Euclid, Ohio. The induction hardened case was achieved using a 10,000 Hz. A.F. motor generator which powered a vertical scanning inductor to raise the surface temperature of the pin to approximately 1600°F. By scanning the pins with the induction coil and spray quench follower at a rate of 0.66 in/sec, a case depth of 0.100 inch was obtained. The self tempered hardness of this pin after induction hardening was Rc 58. This was accomplished by taking advantage of the residual heat in the core of the pin. The final operation in the reprocessing of the pins was the shot peening. This was performed by the Metal Improvement Co. using SAE S330 shot topeen the pins to an Almen strip intensity of 0.011C.

5.2.3. Fatigue Testing

The fatigue testing of tank track pins was conducted using four point bending. The fixturing used in applying four point bending stresses is illustrated in Figure 5-4. The loading source used to apply the loads to the pins was a 20,000 lbs. maximum load Materials Testing System (MTS). This system uses an analog controlled hydraulic pump to power a hydraulic cylinder to apply the loads. The load on the pin is constantly monitored with a load cell connected in series with the hydraulic cylinder and the pin. The MTS controller compares the signal from the load cell with a function generator, to load the pin with the desired wave form. In the testing of the pins, an offset sinusoidal wave was used to produce a low tensile stress, high tensile stress alternating load at a frequency of 10 Hz. This type of loading was chosen to duplicate the testing procedures currently used by the U.S. Army Tank-Automotive Command. This type of loading is also similar to those that might be encountered by the pin during its life cycle because of its positioning in the tank shoe. During the tests, the maximum and minimum loads were periodically checked using either an oscilloscope or the limit detectors. This assured that the pins were being loaded according to the settings on the MTS²⁷.

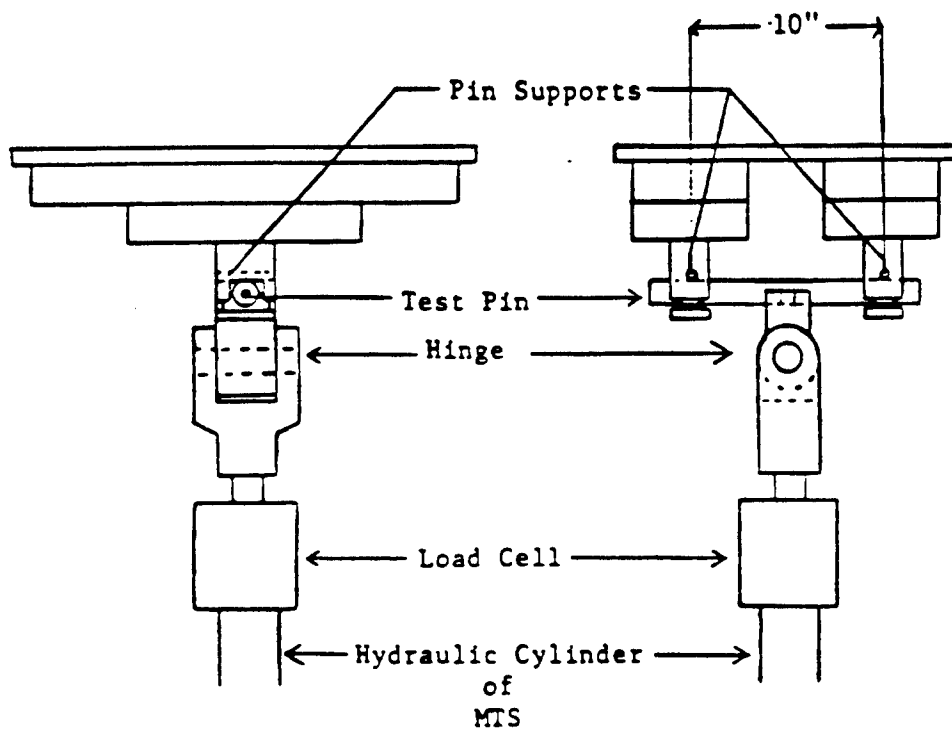


Figure 5-4. The Fixturing of the MTS Used to Fatigue Test Tank Track Pins in Four Point Bending.

Stresses on the outermost fiber (surface) of the pin are calculated using the flexure formula for four point bending as follows :

$$S_{\max} = \frac{M \cdot y}{I}$$

where

M = maximum bending moment (in.-lbs.),

y = distance from neutral axis (in.),

and I = moment of inertia (in.⁴).

Hence,

$$S_{\max} = \frac{8P(L-l)D}{*(D^4-d^4)}$$

where

P = applied load (lbs.),

D = outer diameter of specimen (in.),

d = inner diameter of specimen (in.),

L = outer loading span (in.),

l = inner loading span (in.).

Since L = 10 inches, l = 0.8 inch, D = 1.249 inch, and d = 0.499 inch this equation can be reduced to:

$$S_{\max} = 12.339P$$

The stress calculations were checked by measuring the actual bending stress on the pin when loaded in the MTS. The measurements were made by mounting a temperature compensated strain gage on the midspan position of the pin. The pin was then loaded, and the load versus strain was recorded on an X-Y recorder. The strain measurements were then directly used to determine stress by applying Hooke's law. These results show excellent agreement between measured and calculated stress.

5.2.4. Microhardness Testing

Microhardness traverses were measured across a section from the surface to the inner bore of several pins. Measurements were made on the as received, fatigued, fatigued to failure, reheat treated, and recycled pins. This testing indicates any fatigue hardening or softening that had occurred from fatigue testing. These hardness profiles also provide an exact measure of the induction hardened case depth. This depth is defined by Volume 2 of Metals Handbook as the depth at which the hardness drops to an equivalent Rc 50²⁹. The hardness traverse also evaluates the heat treatment of the pins.

Samples to be tested were sectioned through the midspan point in the region of highest tensile stressing. This transverse section was mounted in bakelite and polished using standard metallographic techniques. The microhardness measurements were obtained on a Leitz Miniload Hardness Tester. Vickers hardness values were measured by applying a load of 1000 g. to a diamond indenter. The Vickers Hardness Number was measured across the section from the O.D to the I.D. at intervals of 0.25 mm. through the induction hardened zone, and 0.50 mm. at deeper locations. A direct Rockwell C hardness was then taken on the sample in the induction hardened zone, core zone and surface for comparison purposes³⁰.

5.2.5. Metallographic Testing

Standard metallography was used for checking the microstructure of the tested pins³¹. As discussed in the literature review, fatigue produces structural changes in materials as fatigue damage accumulates and a crack is formed. By examining as received, fatigued, fatigued to failure, reheat treated, and recycled pins, some of these microstructural changes may be revealed. Since bending fatigue results in a maximum stress gradient at the surface to zero at the neutral axis of the pin, any fatigue damage would be expected near the tensile surface at the O.D. The pins that were examined were sectioned using a water cooled abrasive cut off wheel. The pins were cut so that a longitudinal section through the region of highest tensile stresses could be observed. The samples were then mounted, polished, and etched in Fry's reagent to reveal the microstructure. Fry's reagent consists of 5 g. of CuCl_2 , 40 ml. of HCl, 30 ml. of distilled water, and 25 ml. of ethyl alcohol. It was used to develop the strain lines³¹. Some samples were also examined after etching with 2 percent nital etchant. Observations of the microstructure, along with micrographs, were made at magnifications from 50X to 1500X using a light microscope.

5.2.6. Nondestructive Testing of Tank Track Pins

A very important aspect of the recycling of used tank track pins is whether a crack has developed or is on the verge of developing. Failed pins can be easily found and discarded before reheat treatment, but pins with small microcracks or very high amounts of fatigue damage will not be easily de-

tected. Since high compressive residual stresses are present in the surface from shot peening, any microcracks will be tightly closed until they propagate through the compressive layer. This compressive residual stress could hinder or prevent the detection of microcracks and the possible recycling of cracked pins. These microcracks cannot be eliminated by reheat treatment since this damage is permanent. Pins which have experienced high amounts of fatigue damage may be susceptible to quench cracking in the areas of highest damage. If this damage is not detected during some portion of the reprocessing, it could result in early failure of recycled pins.

All of the pins that were prefatigued were checked for cracks both before and after reheat treatment. This dual inspection method was adopted to establish the source of any cracks. Magnetic particle inspection and liquid penetrant techniques were used to detect any possible cracks. Magnetic particle inspection was conducted using dry Magnaflux, red magnetic particles and a D.C. motor generator welding power supply for the current used in testing. Because the cracks in the pins were expected to be perpendicular to the length of the pins, the magnetic field was induced into the pin perpendicular to the possible cracks. This was accomplished by using loops of copper cable around the pin to induce the magnetic field ³².

Liquid penetrant testing was conducted using a spray dye to indicate cracks. After the pins were cleaned with an organic solvent, the dye was sprayed onto the surface and allowed to penetrate for several minutes. The excess dye is then removed and a developer employed to indicate cracks. Because of surface tension, the cracks retain some of the dye even after the pin is cleaned. It is this retained dye that is indicated when the developer is applied ³².

5.2.7. Statistical Analysis of the Fatigue Data

Statistical analysis was used to evaluate the initial fatigue data to establish the fatigue curve of the pins. The Median Rank Method was employed to obtain the 50 percent probability of failure of the pins at each stress level ². The median rank method has two advantages over numerical averages in analyzing fatigue data. First, it can use all test points, including run out points, in the evaluation of the data. This is important in tests conducted near the endurance limit where some probability exists that a pin will not fail. Second, the Median Rank Method is insensitive to the large scatter inherent in fatigue testing.

The Median Rank Method of analyzing the fatigue data is applied to the set of data at each stress level. The results of all the tests at that level are ordered from shortest to longest lifetime. Each of these lifetimes are then assigned an estimated median rank according to the following equation for a sample size n:

$$\text{Estimated Median Rank} = \frac{0.7}{n+0.4}, \frac{1.7}{n+0.4}, \frac{2.7}{n+0.4}, \dots, \frac{n-0.3}{n+0.4}$$

This number is either the estimated probability of failure, or the estimated percent of failures at this number of cycles. The larger the sample size, the better the estimation will be. The rank versus lifetime data are then plotted as probability versus log of lifetime. A line through these points is then used to determine what the probability of failure is at any number of cycles. The number of cycles that have a 50 percent probability of failure are then used in plotting the S-N curve through the original data ².

5.2.8. Residual Stress Measurement

Surface residual stress measurements were conducted at American Analytical Corp. in Grafton, Ohio. Pins that were in various stages of processing, fatigue testing, overloading, and reprocessing were tested using a Fast-stress residual stress measuring unit. This system automatically performs the Two Angle Method of residual stress measurement which uses X-ray diffraction to determine the residual stresses ³³. The Faststress can measure the surface residual stress of steel parts in 30 seconds.

5.3. RESULTS AND DISCUSSION

The results obtained in this investigation are in four categories: fatigue test results, microhardness test results, metallographic results and residual stress measurement results. The data compiled in each of these categories will be presented first, then the integration of these results will be discussed.

5.3.1. Fatigue Test Results

The results of the fatigue testing of the tank track pins are listed in Tables 5-2 through 5-4. These tables report the number of cycles of reverse bending which caused failure at a given stress. These results are plotted in Figures 5-5 through 5-7. Figures 5-5 and 5-7 show the S-N curves for the pins in the as received and reheat treated conditions, respectively and Figure 5-6 shows the base curve of the as received pins, based on a statistical evaluation of the original data. Figure 5-8 illustrates the base curve, the reheat treated curve, and the recycled points plotted together for comparison.

5.3.1.1. As Received Pins. The fatigue testing of as received tank track pins resulted in the establishment of the base S-N curve shown in Figure 5-5 and Table 5-2. At least five tests were conducted at each of eight different stress levels to establish this fatigue curve. The S-N curve is drawn through the points which represent the 50 percent probability of failure of the pins as defined previously. The statistical evaluation of the raw data (Table 5-2), using the Median Rank Method, is shown in Table 5-5. The probability of failure versus cycles to failure at each stress level is plotted in Figure 5-9. Figure 5-6 indicates the statistical S-N

Table 5-2. Results of Bending Fatigue Tests Conducted on as Received, T-142 Tank Track Pins. The Stresses are Calculated from Strain Gage Measurements. The 'R' Value (S_{\min}/S_{\max}) is 0.03. The Frequency is 10 Hz.

Maximum Stress (ksi)	Cycles to Failure			
209	14,000 26,350	17,210 35,350	20,000	20,890
194	31,490 50,000	33,870	38,370	42,700
181	62,280 91,370	79,010 105,900	83,740 107,190	87,040 110,180
175	80,900 172,800	86,180 224,500	89,560* DNF	120,804
169	90,310 217,280	126,770 467,000	146,810	153,080
167	92,000 208,270* DNF	137,450 353,550* DNF	150,000 369,780	178,560* DNF
162	118,900 285,000* DNF	128,700 321,000* DNF	163,300 324,800	209,900* DNF
155	DNF*	DNF*	DNF*	

*Did Not Fail in 2,000,000 cycles.

Table 5-3. Results of Bending Fatigue Tests Conducted on Reheat Treated Tank Track Pins. The 'R' Value is 0.03, and the Testing Frequency, 10 Hz.

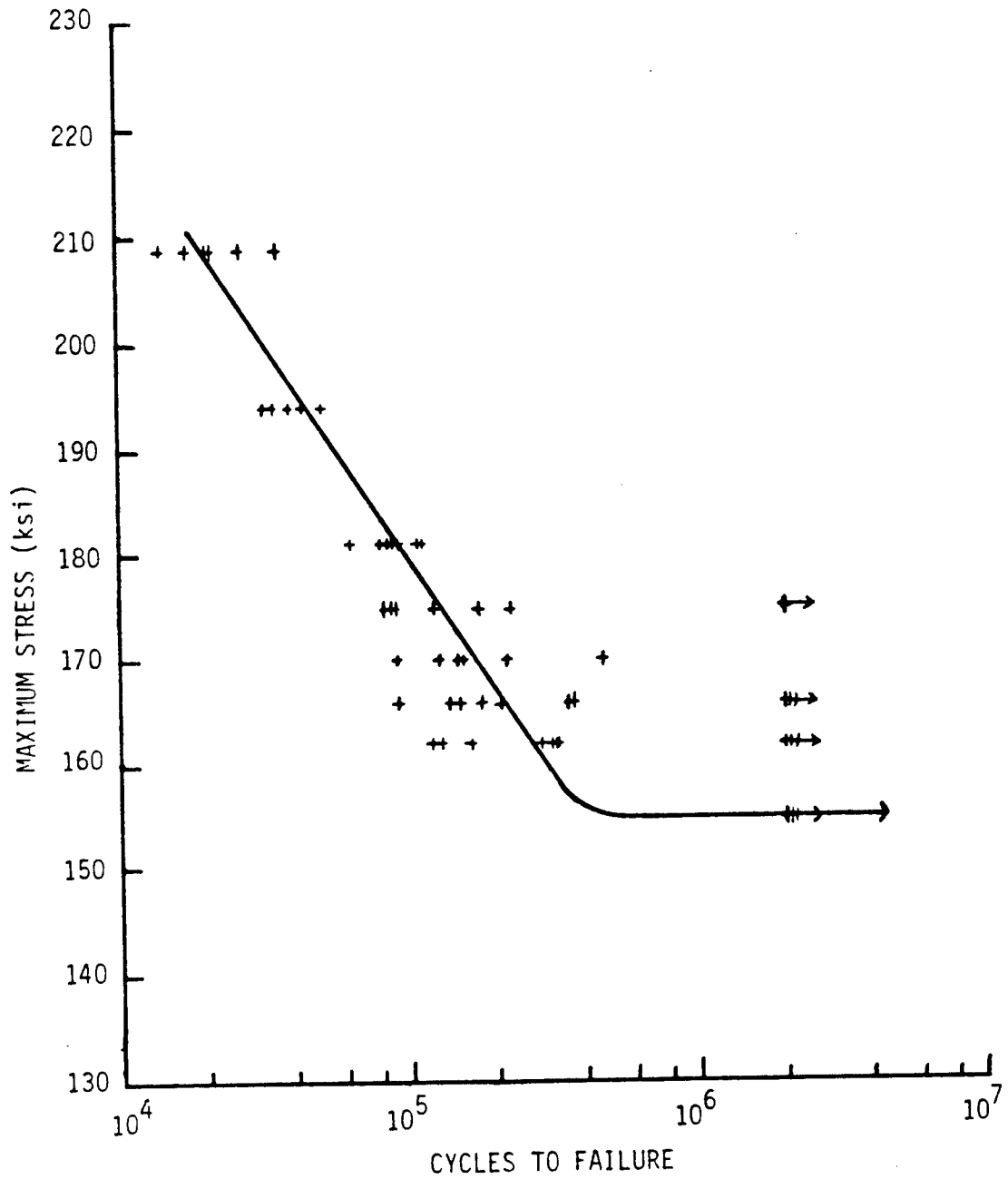
<u>Maximum Stress (ksi)</u>	<u>Cycles to Failure</u>
194	102,830
181	177,330
170	296,940
166	DNF*

* Did Not Fail in 2,000,000 cycles.

Table 5-4. Results of Bending Fatigue Tests Conducted on Fatigued and Reheat Treated Tank Track Pins. The 'R' value is 0.03, and the Testing Frequency, 10 Hz.

<u>Maximun Stress (ksi)</u>	<u>Initial Cycles</u>	<u>Cycles to Failure</u>
194	38,000	69,660
	30,000	85,560
181	71,110	143,450
175	70,000	DNF*
	70,000	159,750
167	100,000	408,270
	100,000	350,030
162	DNF*	DNF*
160	DNF*	DNF*

*Did Not Fail in 2,000,000 cycles.



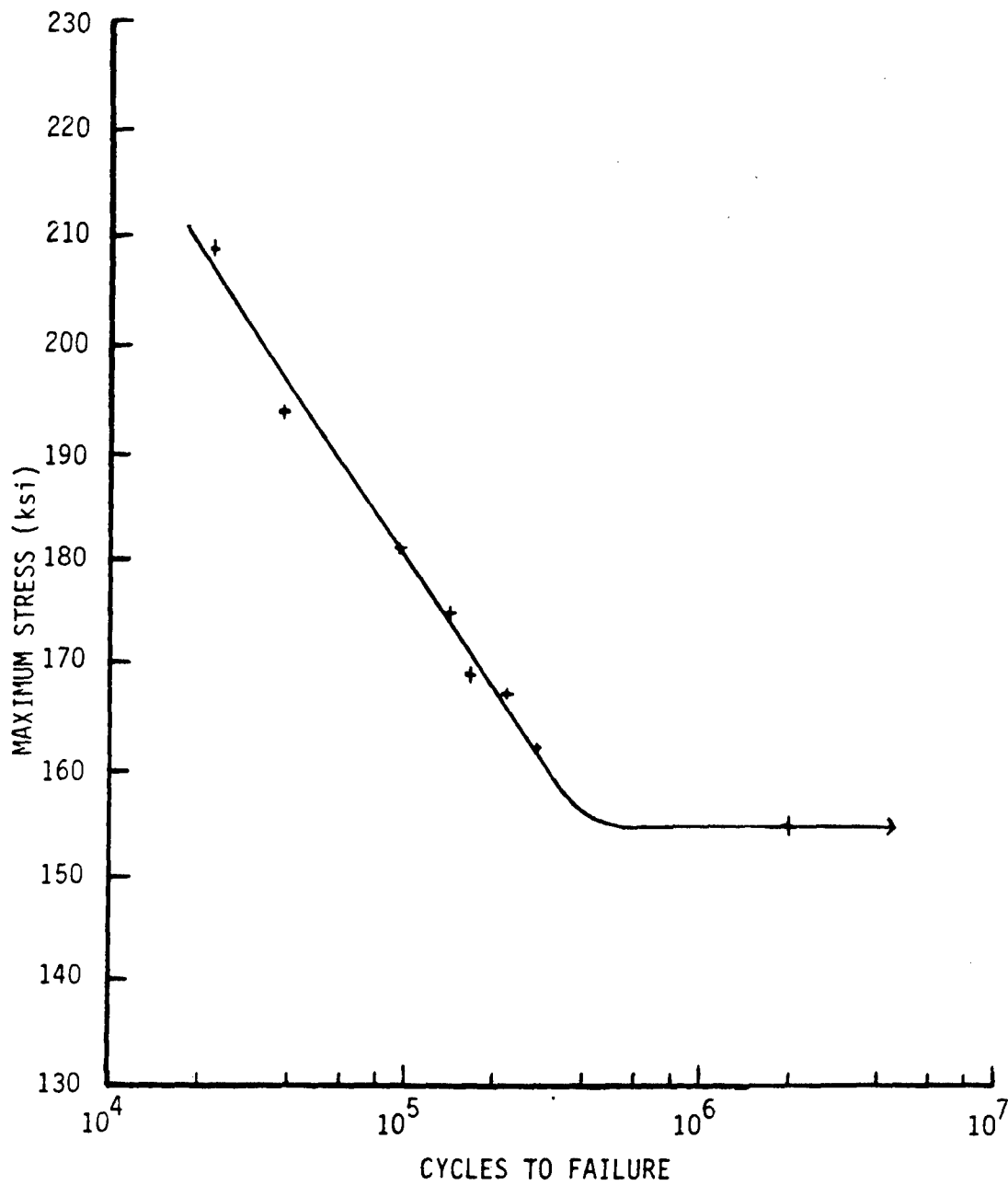


Figure 5-6. A Plot of the Statistical S-N Curve of the as Received Tank Pins.

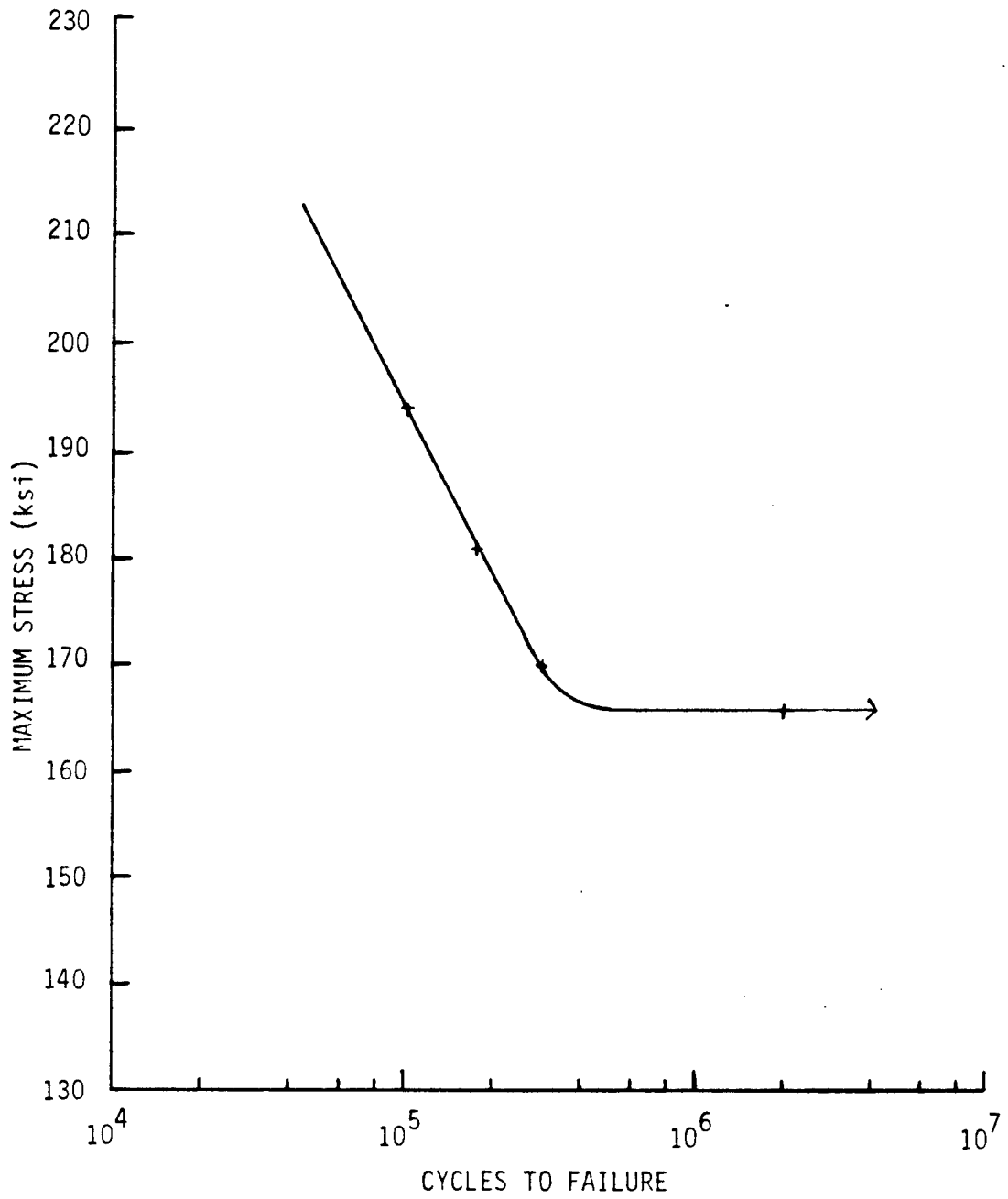


Figure 5-7. A Plot of the Data and the S-N Curve of Tank Track Pin T-142 After Reheat Treatment. Testing was Conducted Using Four Point, Tensile-Tensile Bending Fatigue, with a 'R' Value of .03 and Test Frequency of 10 Hz.

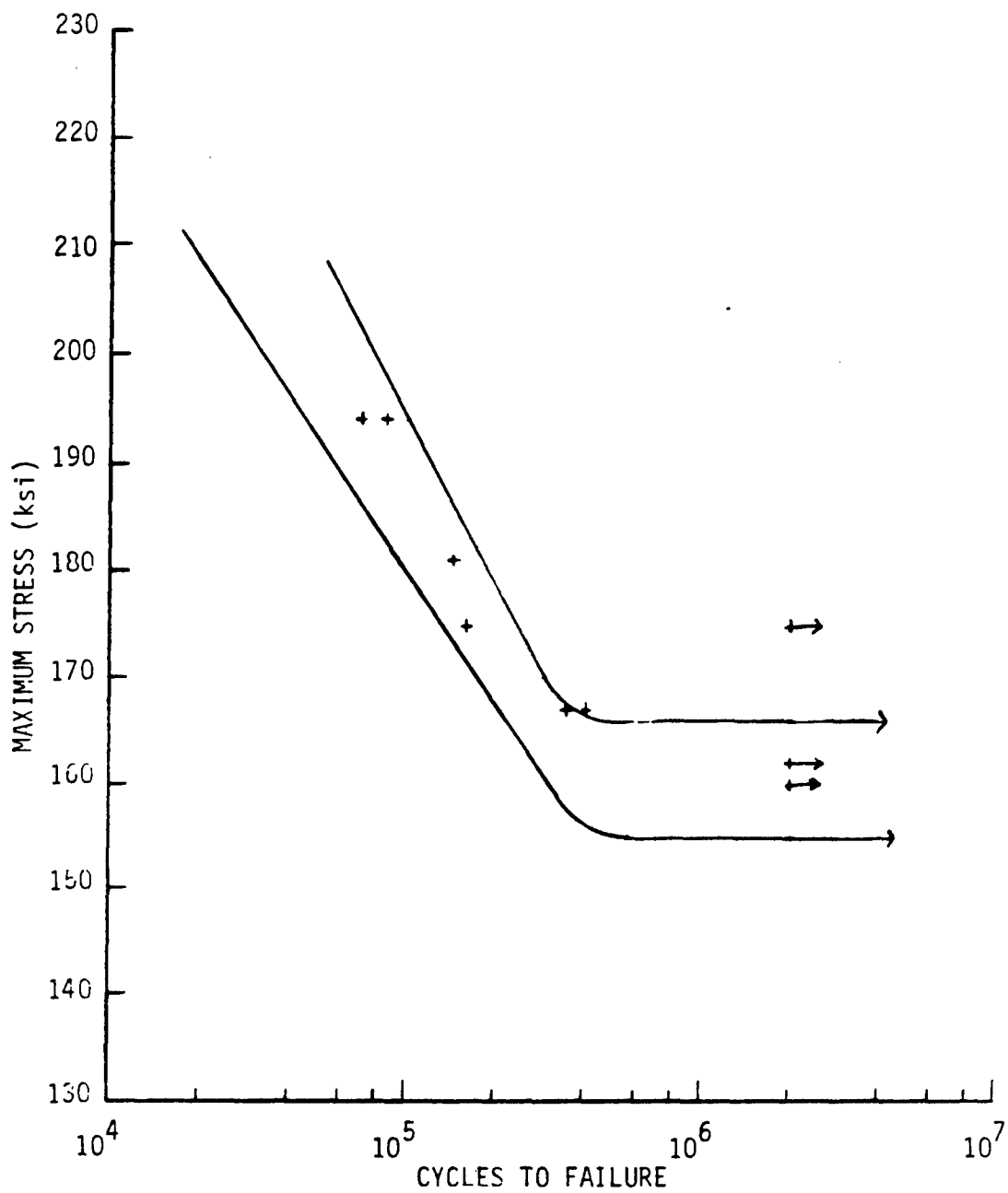


Figure 5-8. The S-N Curves of As Received and Reheat Treated Tank Track Pin T-142 Along With Data Points from Fatigue Testing of Recycled Pins Shown as '+'.

Table 5-5. Results of Microhardness Traverses Through Tank Track Pins From Surface to I.D. at Various Stages of Testing.

DEPTH (mm.)	AS RECEIVED VHN	FATIGUED 80% VHN	FATIGUED TO FAILURE VHN
0.25	672	636	675
0.50	750	596	668
0.75	750 (RC 58)	636 (RC 57)	656 (RC 57)
1.00	672	639	656
1.50	672	619	646
1.75	672*	570*	500*
2.00	492	347	345
2.25	345	370	390
2.50	376	386	411
2.75	396	370	410
3.00	396	420	415
3.50	425	428	422
4.00	432	428	422
4.50	432 (Rc 43)	428 (Rc 43)	434 (Rc 44)
5.00	417	428	438
6.00	417	418	459
7.00	417	428	471
8.00	417	432	470
9.00	417		
9.50	417		

* Case Depth defined as Rc 50 (= 510₂VHN)

VHN - Vickers Hardness Number (kg/mm²)

Rc - Hardness Rockwell C-scale

Table 5-5. Results of Microhardness Traverses Through
 (continued) Tank Track Pins From Surface to I.D. at Various Stages
 of Testing.

DEPTH (mm.)	REHEAT TREATED VHN	RECYCLED VHN
0.25	672	630
0.50	672	674
0.75	690 (Rc 59)	672 (Rc 59)
1.00	690	674
1.50	722	690
1.75	672	674
2.00	672	672
2.25	672*	605*
2.50	323	340
2.75	417	361
3.00	403	351
3.50	417	403
4.00	400	426
4.50	417 (Rc 45)	439 (Rc 45)
5.00	425	450
6.00	425	440
7.00	448	450
8.00	448	470
9.00	448	462
9.50	417	450

* Case Depth defined as Rc 50 (= 510 VHN)

VHN - Vickers Hardness Number (kg/mm²)

Rc - Hardness Rockwell C-scale

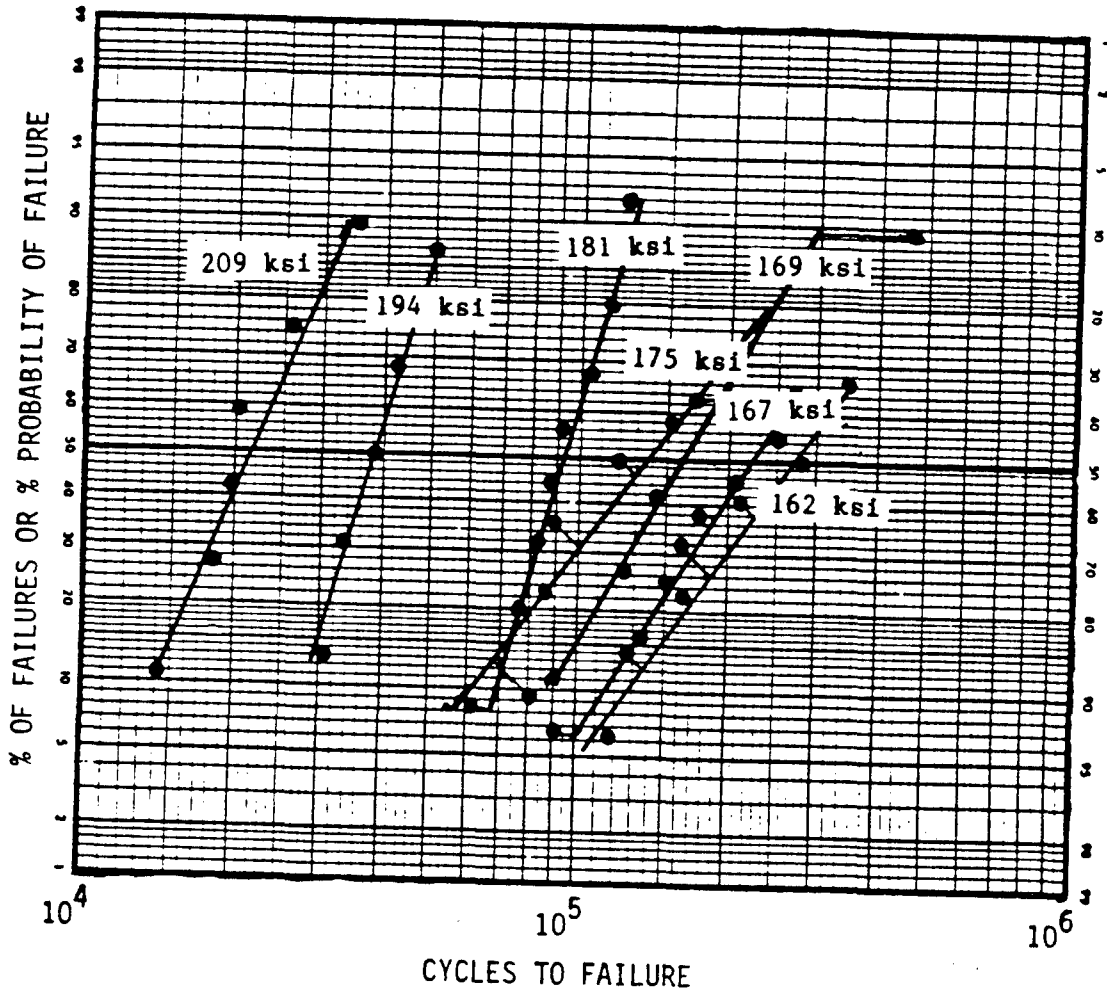


Figure 5-9. The Plot of the Statistical Median Rank of Fatigue Data on as Received Pin at Different Stress Levels.

curve for the as received pins without the data points in a convenient form for comparative purposes. The S-N curve demonstrates that the endurance limit for the as received pins is 155 ksi. It also shows that considerably more variation occurs in lifetime data at stress levels just above the endurance limit than at much higher stresses.

During the fatigue testing of the pins, it was observed that a high pitched audible "ping" occurred several hundred cycles before the pins failed. It was believed that the cause of this "ping" was the advancement of a crack in the pin. To check this, several tests were monitored using the MTS's Linear Variable Differential Transformer (LVDT) to measure the deflection of the pin during fatigue loading. Since the testing is conducted at high frequencies, an oscilloscope was employed to monitor the LVDT. It was observed that the "ping" corresponded to a significant increase in the deflection of the pin in one cycle. This change in deflection occurs because of a propagating crack which reduces the cross section being loaded, thereby increasing the stress and strains in the remaining area. A gradual change in pin deflection would indicate slow crack growth, but, as occurred, a rapid change in the pin deflection indicates fast crack propagation. Another check of this observation was made by stopping the fatigue test within 20 cycles after the "ping" occurred and sectioning the pin through the region of highest stress. A metallographic specimen of this area was mounted in bakelite and polished. Figure 5-10, an unetched micrograph of this area, shows that a crack has propagated from the surface of the pin. The crack shows two stages of growth. The first stage is at 45° to the surface of the pin along the maximum shear stress plane. This crack continues from the surface to a depth of 0.010 inch. No noticeable change in the deflection of the pin occurred to indicate this first stage of crack growth. From this point, the crack propagates along a plane normal to the maximum stress axis to the end of the induction hardened zone. The transition to this stage appears to occur when the crack propagates below the layer of compressive residual stresses near the surface. This location in the pin under the residual compressive stress layer has high net tensile stresses. The second stage of crack propagation is slowed considerably when the crack reaches the softer and ductile transition zone between the case and core as shown by subsequent microhardness results, at a depth of 0.100 inch. Figure 5-11 is a light fractograph which demonstrates a typical fracture surface of an as received pin. The arrow points to the origin of the crack at the outer surface of the pin. From this point, the crack propagated around the circumference of the induction hardened zone and across the core region, as indicated by the chevron lines.

The results of these initial tests on as received production pins were used to choose the stress levels and number of stress cycles to be applied to the pins before recycling. The number of cycles of prefatigue was generally set at 80 percent of the lowest lifetime observed at a given stress level; occasionally this caused the failure of a pin. When this occurred, subsequent pins were tested to 80 percent of this new lowest lifetime.

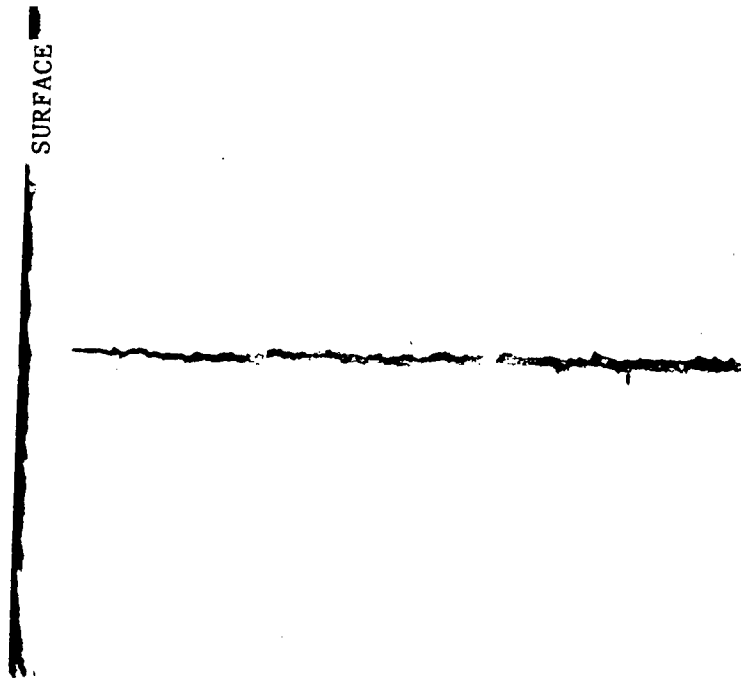


Figure 5-10. An Unetched Micrograph of the Surface of an As Received Pin After 23,851 Cycles at a Stress of 184 ksi Showing a Fatigue Crack Which Has Propagated Through the Induction Hardened Layer. Fatigue Testing Was Stopped After a High Pitched Pping" Indicated the Growth of the Crack. Magnification 40X.



Figure 5-11. A Fracture Surface of an As Received Tank Track Pin. The Arrow Points to the Fracture Origin at the Outer Surface.

5.3.1.2. Reheat Treated Pins. Four pins were reheat treated without having been fatigued to provide an indication of the fatigue characteristics of an nondamaged pin. The results of these tests are shown in Figure 5-7 and Table 5-2. Since only one pin was tested at each stress level, it is defined by the Median Rank Method as the 50 percent probability of failure. This does not represent a significant statistical analysis. The S-N curve drawn through the resultant points in Figure 5-7 shows the endurance limit to be 166 ksi. This fatigue limit is significantly higher than for the as received pins. The improvement in fatigue properties of the reheat treated pins is attributed to the combined effect of a slightly higher case and core hardness, a deeper case depth, and a slight carburization of the surface from the controlled carbon heat treatment. The surface hardnesses of the reheat treated pins were measured to be in the range of Rc 59 to 60, whereas, the hardnesses of the as received pins were between Rc 57 and 58. The case depth of the reheat treated pins is indicated in the microhardness data (Table 5-5) as the depth where the hardness drops below an equivalent Rc 50 (=510 DPH). This depth was measured to be 0.100 inch for the reheat treated pins, and 0.090 inch for the as received pins. This difference in case depths is significant although both values are within the specification range (0.060 + 0.060 inch). The possibility of the carburization of the reheat treated pins is not indicated in the microhardness measurements but was revealed in the metallographic examination of the pins.

The improved fatigue properties of the reheat treated pins cannot be attributed to higher compressive residual stresses in the reheat treated pin from shot peening. Table 5-6 shows that the measured residual stresses are in fact lower in the reheat treated pins. The effect of shot peening on fatigue behavior is influenced by other factors in addition to the high compressive residual stresses in the surface layer. Shot peening also produces surface roughness and this reduces the fatigue resistance by creating notches which act as stress concentrators and sources of crack nucleation. Previous work has demonstrated that a considerable reduction in the endurance limit of steels occurs at high hardness levels from surface roughness². Although the reshot peening of the pins was within the Almen strip specification at 0.011C, it was accomplished using a slightly smaller shot size of S330 that produces a smoother surface and less stress concentration from notching. The reheat treated pins were also processed under rigid atmosphere control and this may have resulted in their better performance.

The origin of the fatigue crack in the reheat treated pins was at the outer surface of the pin in the highest tensile region; this is the same location as for the as received pins. A typical fracture surface of a reheated pin is shown in Figure 5-12, with the crack origin indicated by the arrow.

5.3.1.3. Recycled Pins. Recycled pins are those which were fatigued just short of failure and then reprocessed. The fatigue test results of these pins, conducted at six different stress levels, are listed in Table 5-4 and plotted along with fatigue curves for the as received and reheat treated pins in Figure 5-8. These data indicate that the recycled pins have better fatigue properties than the original production pins but do not quite at-

Table 5-6. The Statistical Evaluation of the As Received Pin Fatigue Data Using the Median Rank Method. The Estimated Rank Represents the Probability of Failure or Percent Failures in the Corresponding Number of Cycles.

Stress: 209 ksi	
Lifetime (N_f)	Estimated Rank (%)
14,000	11
17,210	27
20,000	42
20,890	58
26,350	73
35,350	89

Stress: 194 ksi	
Lifetime (N_f)	Estimated Rank (%)
31,490	13
33,870	31
38,370	50
42,700	69
50,000	87

Stress: 181 ksi	
Lifetime (N_f)	Estimated Rank (%)
62,280	8
79,010	20
83,740	32
87,040	44
91,370	56
105,900	68
107,190	80
110,180	

Stress: 175 ksi	
Lifetime (N_f)	Estimated Rank (%)
80,900	9
86,740	23
89,740	36
120,804	50
172,800	64
224,500	77
DNF	91

Table 5-6. The Statistical Evaluation of the As Received
 (Continued) Pin Fatigue Data Using the Median Rank Method.
 The Estimated Rank Represents the Probability
 of Failure or Percent Failures in the Corre-
 sponding Number of Cycles.

Stress: 169 ksi		Stress: 167 ksi	
Lifetime (N_f)	Estimated Rank (%)	Lifetime (N_f)	Estimated Rank (%)
90,310	11	92,000	7
126,770	27	137,450	16
146,810	42	150,000	26
153,080	58	178,560	36
217,280	73	208,270	45
467,000	89	353,550	55
		369,780	64
		DNF	74
		DNF	84
		DNF	93

Stress: 162 ksi		Stress: 155 ksi	
Lifetime (N_f)	Estimated Rank (%)	Lifetime (N_f)	Estimated Rank (%)
118,900	7	DNF	21
128,700	16	DNF	50
163,300	26	DNF	79
209,900	36		
285,000	45		
321,000	55		
324,800	64		
DNF	74		
DNF	84		
DNF	93		

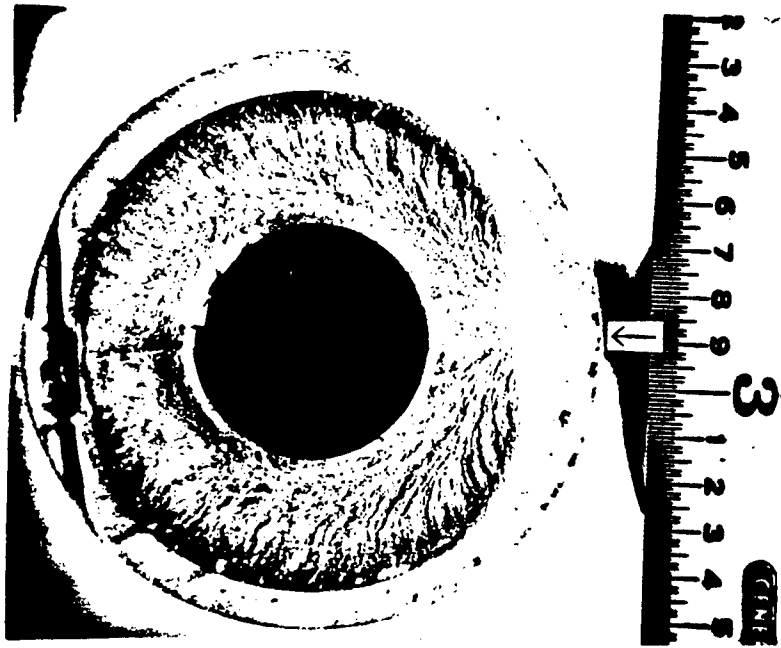


Figure 5-12. A Typical Fracture Surface of a Fatigued Pin That Had Undergone Reheat Treatment.

tain the fatigue strength of the reheat treated pins. This indicates that some small permanent fatigue damage may be present as a result of fatiguing that is not eliminated by reheat treatment.

Although the above test results show a marked improvement in fatigue properties after reheat treatment for most fatigued pins, a few pins that contained surface cracks from previous testing or reheat treatment failed prematurely. The existence of a crack prior to the final fatigue testing was indicated by a small zone containing a dark oxide scale on the fracture surface, at the crack origin. To determine whether the crack was a result of prefatigue testing or from quenching, a metallographic section was taken through the origin of the crack. This examination showed the crack to be perpendicular to the surface which can be seen in Figure 5-13. For this reason it is believed that the crack resulted from the reheat treatment, and most probably from quenching which developed high tensile stresses in the surface. The lack of detection of these cracks by NDT is attributed to crack closure from the high compressive residual stresses from induction hardening and shot peening.

5.3.2. Microhardness Test Results

5.3.2.1. As Received Pins. The microhardness profile of an as received pin from the surface to the bore is shown in Figure 5-14 and the data listed in Table 5-5. The profile demonstrates three regions: the induction hardened case, a soft transition zone, and a medium hard core. The hardness of the core results from the initial quench and temper and is 43 Rc. The hardened case from induction hardening has an average hardness of 58 Rc. This zone extends in from the surface to a depth of 0.090 inch. The transition zone is also a result of induction hardening. During induction hardening, a cold pin is brought to a surface temperature of 1600^oF within seconds. As the pin is scanned, it is quenched to transform the structure to a high hardness martensite. The core of the pin remains at a relatively low temperature throughout the procedure. However, the region between these two zones is not heated into the upper critical temperature region and receives a high temperature temper from the thermal gradient. This produces the low hardness values that were observed in the profile.

5.3.2.2. Fatigued Pins. The microhardness profiles of pins fatigued to roughly 80 percent of their expected life and to failure are plotted in Figures 5-15 and 5-16 from the data in Table 5-5. These profiles show a similar hardness pattern as the as received pins. It was noted that these profiles do not show any fatigue softening as reported elsewhere ⁶. The hardness of the case is 57 Rc for both the 80 percent fatigued and failed pin. The core hardness is also virtually the same for each case at 43 Rc and 44 Rc, respectively.

5.3.2.3. Reheat Treated Pins. Two sets of reheat treated pins were tested by a microhardness traverse. The first set of tests were conducted on pins that were only reheat treated, as shown in Figure 5-17 and Table 5-5. This microhardness profile indicates that the reheat treatment was conducted



Figure 5-13. A Micrograph Showing the Cross Section of the Crack Origin of a Recycled Pin That Failed Prematurely. The Crack Propagated Perpendicularly From the Surface Indicating That the Crack Is Probably From Quenching Rather Than Fatigue Stressing. 40X. Unetched. $N_i=200,000$ Cycles. $N_f=54,000$ Cycles.

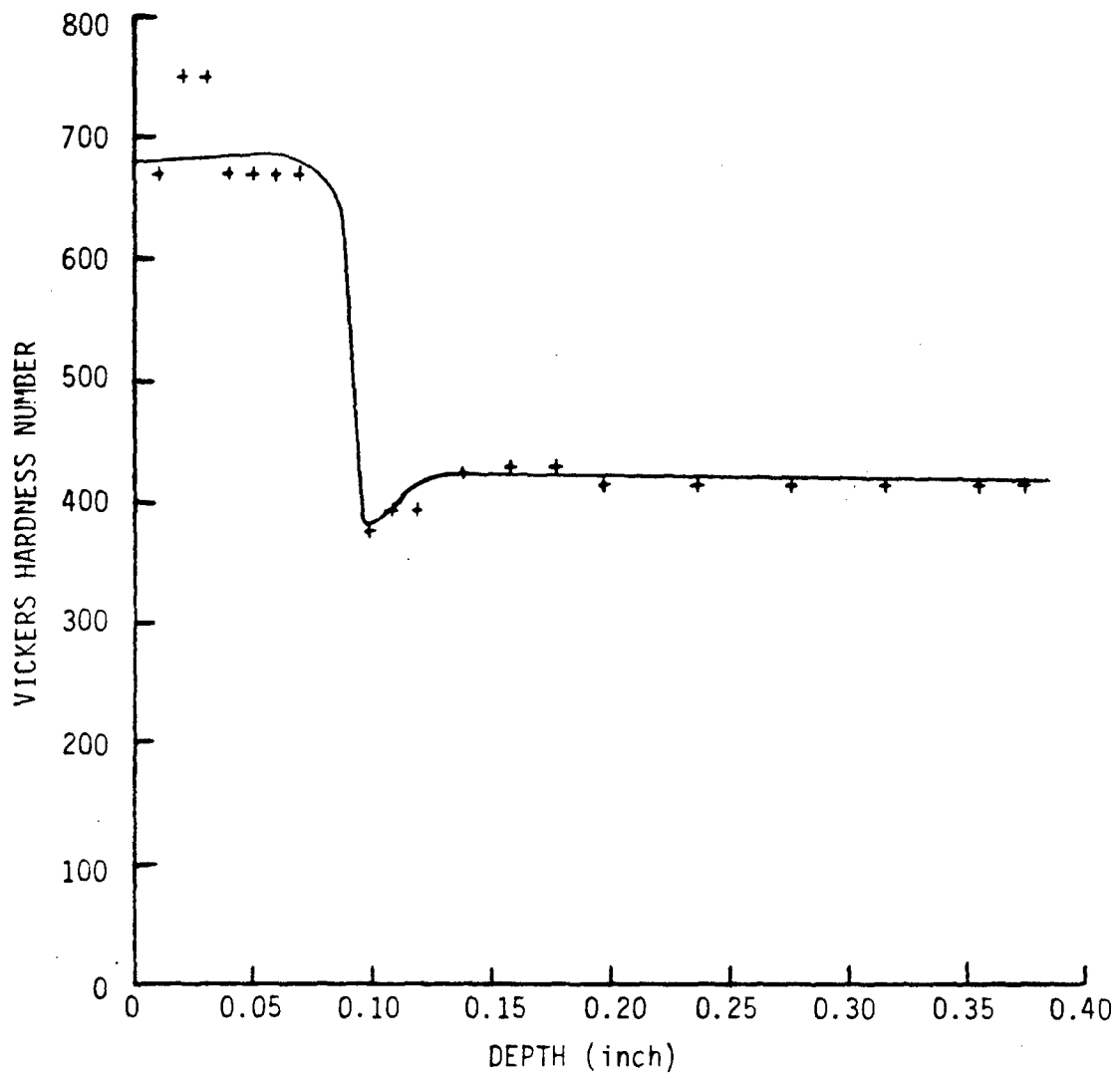


Figure 5-14. Hardness Traverse from the O.D. to the I.D. of Tank Track Pin T-142 As Received. The Surface Hardness Was Rc 58, and the Core Hardness Rc 43.

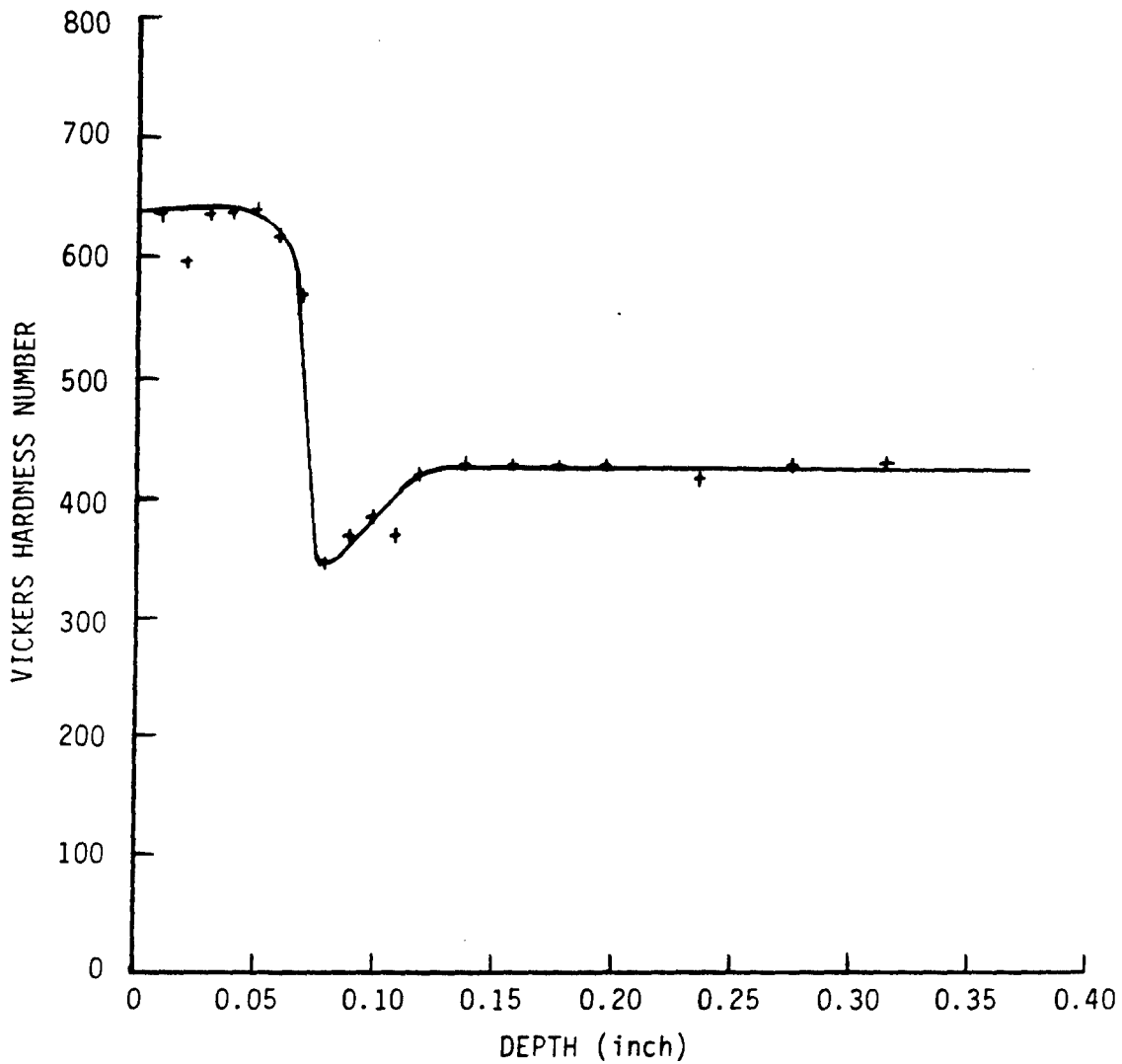


Figure 5-15. Hardness Traverse From the O.D. to the I.D. of Tank Track Pin T-142 After Fatigue Cycling to 80 Percent of Expected Life. The Surface Hardness was Rc 57, and the Core Hardness Rc 43.

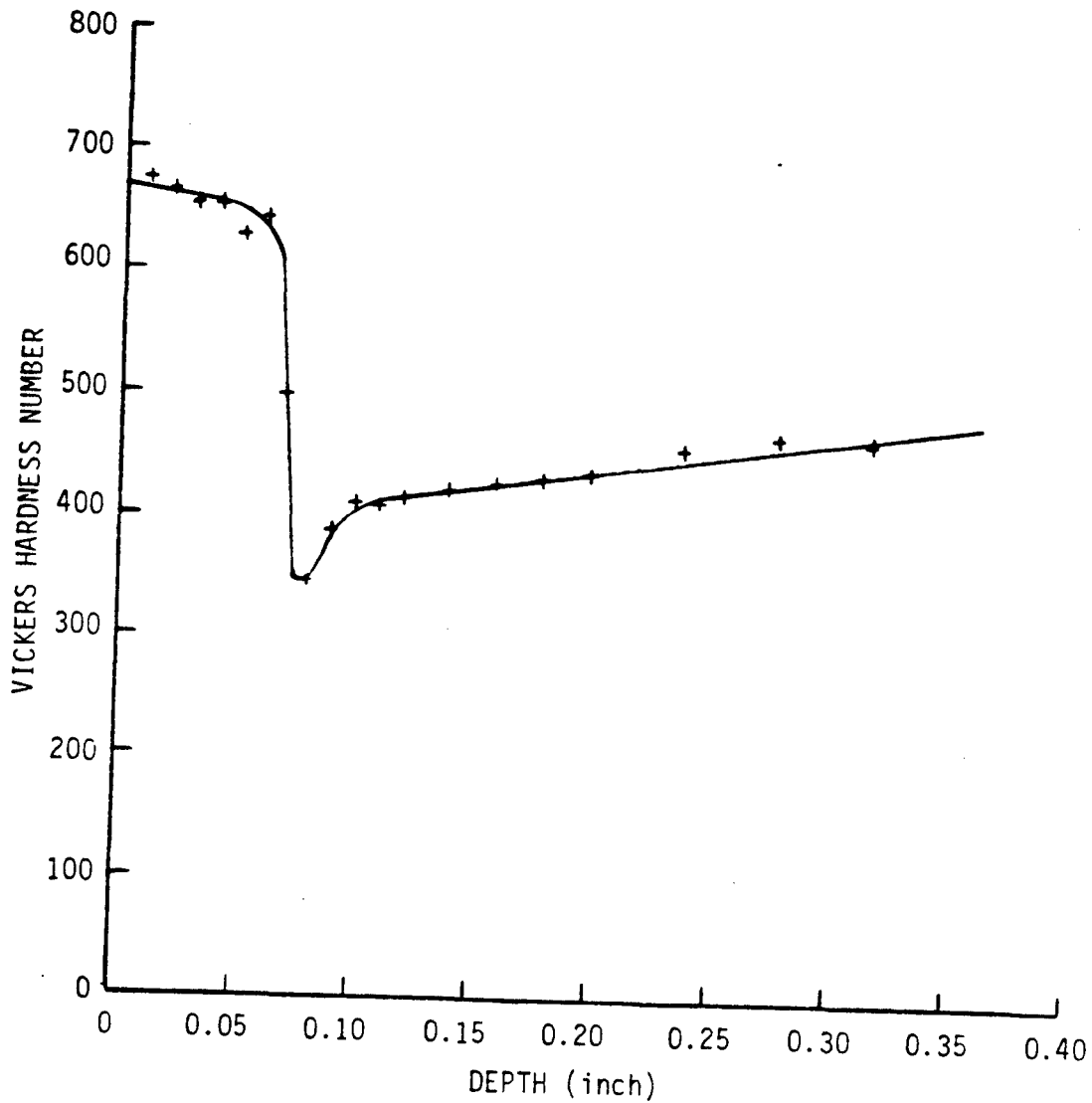


Figure 5-16. Hardness Traverse From the O.D. to the I.D. of Tank Track Pin T-142 After Being Fatigued to Failure. The Surface Hardness Was Rc 57, and the Core Hardness Rc 44.

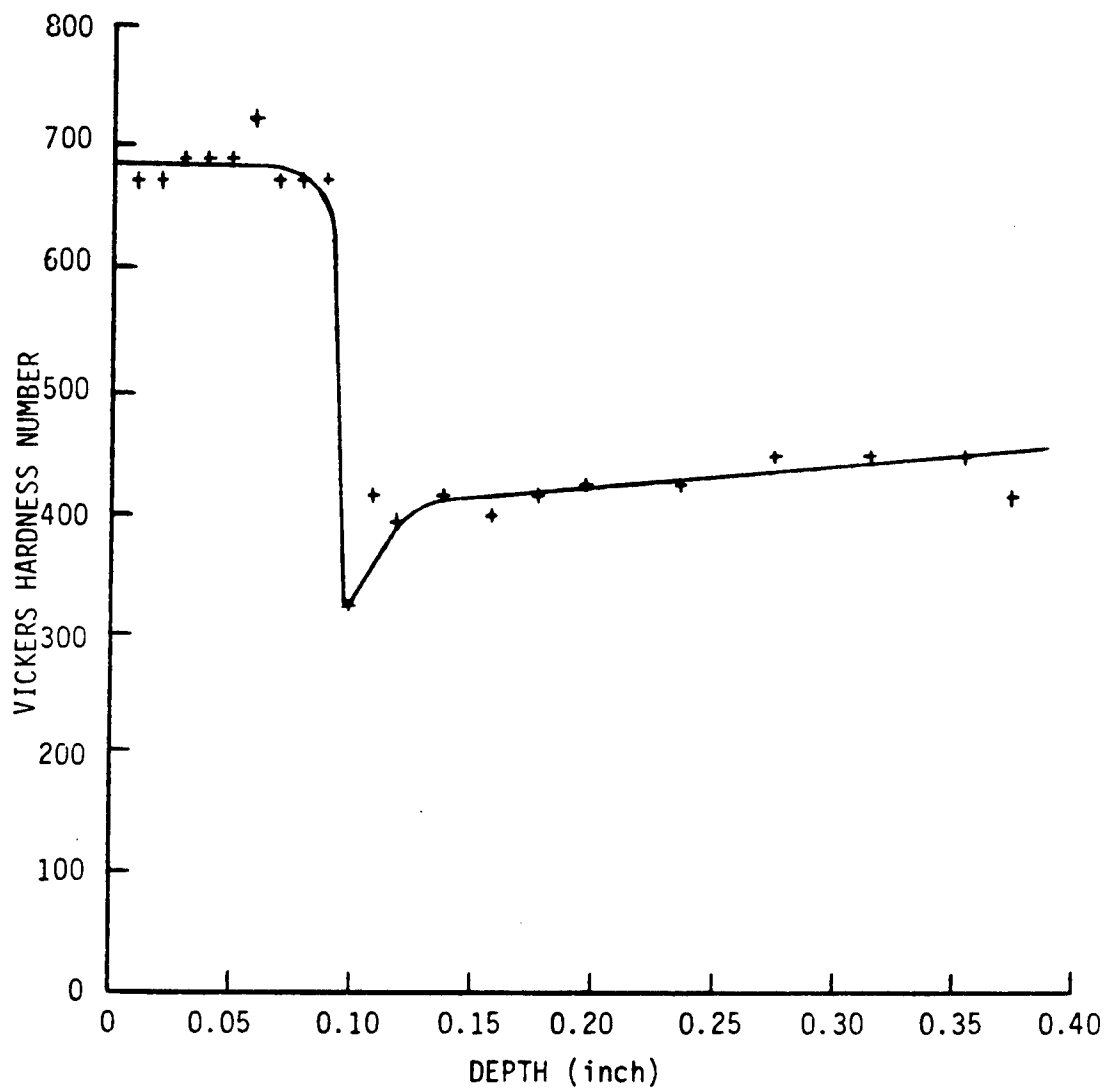


Figure 5-17. Hardness Traverse From the O.D. to the I.D. of Tank Track Pin T-142 After Reheat Treatment. The Surface Hardness Was Rc 59, and the Core Hardness Rc 45.

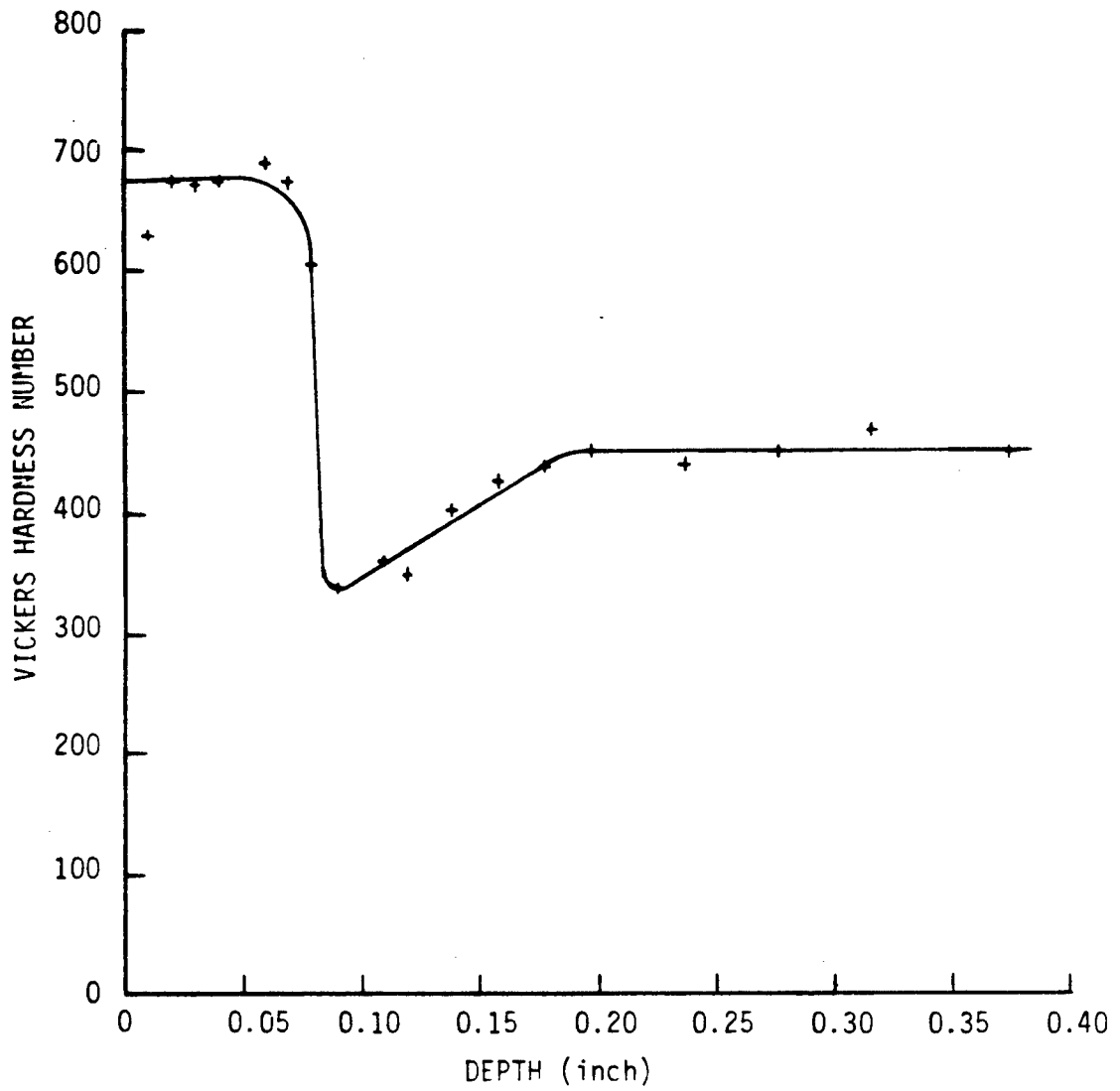


Figure 5-18. Hardness Traverse From the O.D. to the I.D. of Tank Track Pin T-142 Which Was Subjected to Fatigue Stressing and Then Recycled. The Surface Hardness Was Rc 59, and the Core Hardness Rc 45.

within the specifications with a case hardness of Rc 59 to a depth of 0.100 inch, and a core hardness of Rc 44. This result is very similar to that of the as received pins. No indication of any reduced hardness at or near the surface was noted. Decarburization during the heat treatment was prevented by heat treating in a carbon controlled gas furnace. The microhardness results of the recycled pins are shown in Figure 5-18 and Table 5-5. These results are virtually identical to those of the reheat treated pins with a case hardness of 59 Rc, case depth of 0.100, and core hardness of 45 Rc.

5.3.3. Metallographic Results

5.3.3.1. As Received Pins. The microstructure of the as received pins illustrates two main constituents; the microstructure in the induction hardened zone shown in Figure 5-19 is fine martensite; the core structure shown in Figure 5-20 is tempered martensite. A low magnification micrograph is included in Figure 5-21 demonstrating the transition from the induction hardened to quenched and tempered microstructure.

5.3.3.2. Fatigued Microstructure. Figure 5-22 is a high magnification micrograph taken at the surface of a fatigued pin. Some evidence of slip banding is indicated by the arrow. Such banding is expected since similar observations have been made by authors on other fatigued structures²⁴. Slip banding results from microplastic strains in areas of maximum tensile stresses and along the maximum shear stress directions. In tank track pins with high compressive residual surface stresses, the maximum net tensile region would be near or slightly below this outer surface. The rest of the microstructure is the same as that of the as received pins. This is expected since no other macrostructural changes would be expected from fatigue testing.

5.3.3.3. Reheat Treated Pins. The microstructure of the reheat treated pins is similar to that of the as received pins. It consists of the same fine martensite at the outer surface in the induction hardened zone, and a coarser tempered martensitic core zone. Figure 5-23 illustrates the structure of the surface at high magnification. A small spheroidal, carbide network is present at the surface which extends into the pin to a depth of 0.001 inch. This network is attributed to the carbon controlled heat treatment used in reprocessing. This type of microstructure was not present before reheat treatment. The pins that were recycled after being subjected to fatigue stressing showed the same microstructure as the reheat treated pins. No evidence of slip banding was observed after the reheat treatment of the fatigued pins.

5.3.4. Surface Residual Stress Results

5.3.4.1. As Received Pins. The results of the residual stress measurements that were taken on the surface of tank track pins are summarized in Table 5-7. The as received pins showed a surface residual stress of -110 ksi. This value corresponds to what would be approximately one half the yield strength of the material. Testing of an as received pin that had not



Figure 5-19. The Microstructure of an As Received Pin Showing The Induction Hardened Zone Which Consists of Fine Self-Tempered Martensite. 500X. Nital Etch.



Figure 5-20. The Core Microstructure of an As Received Pin Showing Coarse Tempered Martensite. 500X. Nital Etch.

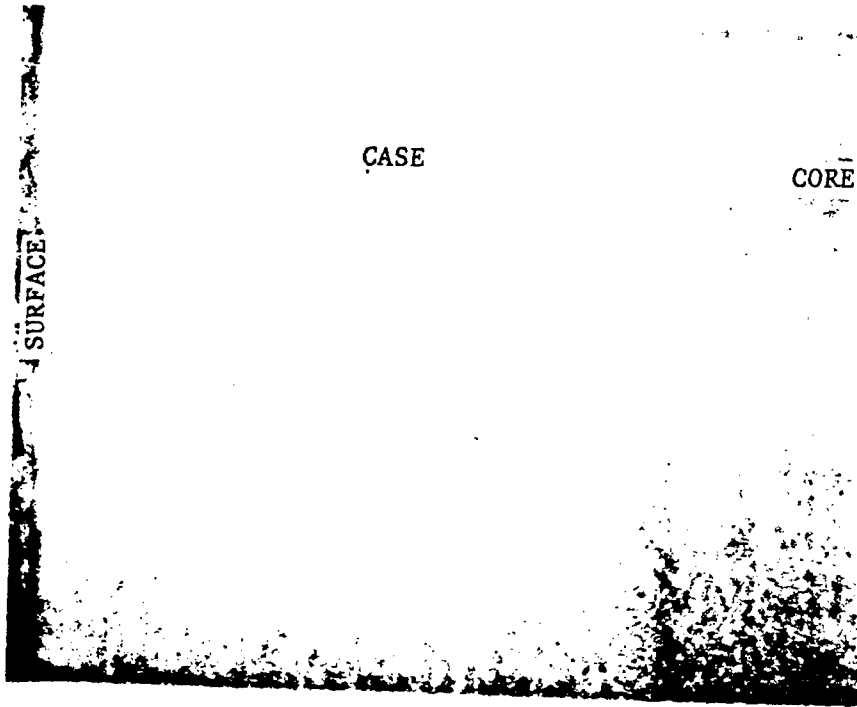


Figure 5-21. A Micrograph Showing the Transition Zone Between Figures 5-19 and 5-20. 40X. Nital Etch.

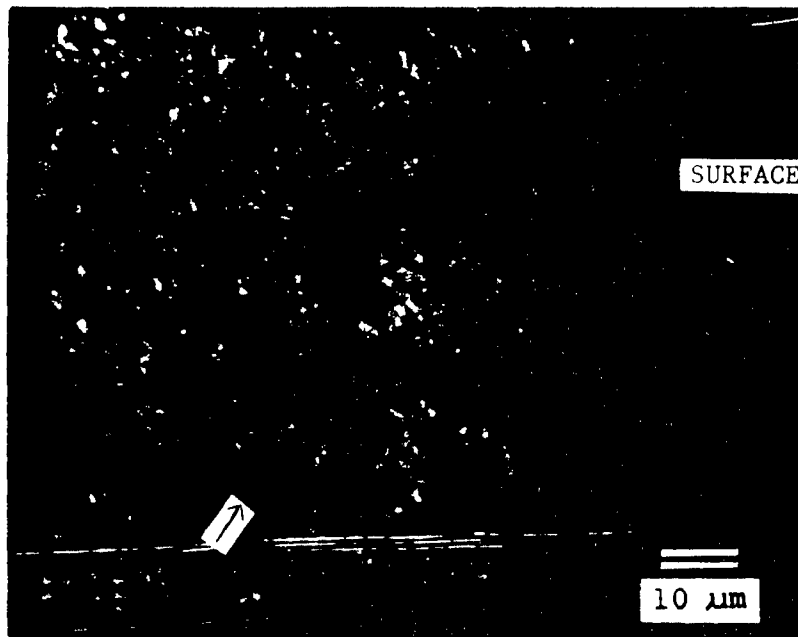


Figure 5-22. A Micrograph of the Surface of a Fatigued, But Not Failed Tank Track Pin. The Arrow Shows Regions of Slip Banding. $N_f = 112,440$ Cycles. $S_{max} = 167$ ksi. 1500X. Fry's Reagent.

Table 5-7. Results of Residual Stress Measurements of Tank Track Pins in Various Conditions. Measurements Were Made With a Faststress Residual Stress Measuring Unit at American Analytical Corporation of Grafton, Ohio.

<u>Condition</u>	<u>Residual Stress</u>
As Received #1	-110 ksi.
As Received #2	-110 ksi.
As Received, without shot peening	-15 ksi.
As Received, loaded with single 345 ksi. bending stress	-68 ksi.
As Received, fatigued 1.8 million cycles at 149 ksi maximum stress	-110 ksi.
Fatigued to crack, 0.25 inch from crack in highly stressed region	-90 ksi.
Fatigued to crack, at crack (lowest value)	-32 ksi.
Reheat treated	-90 ksi.

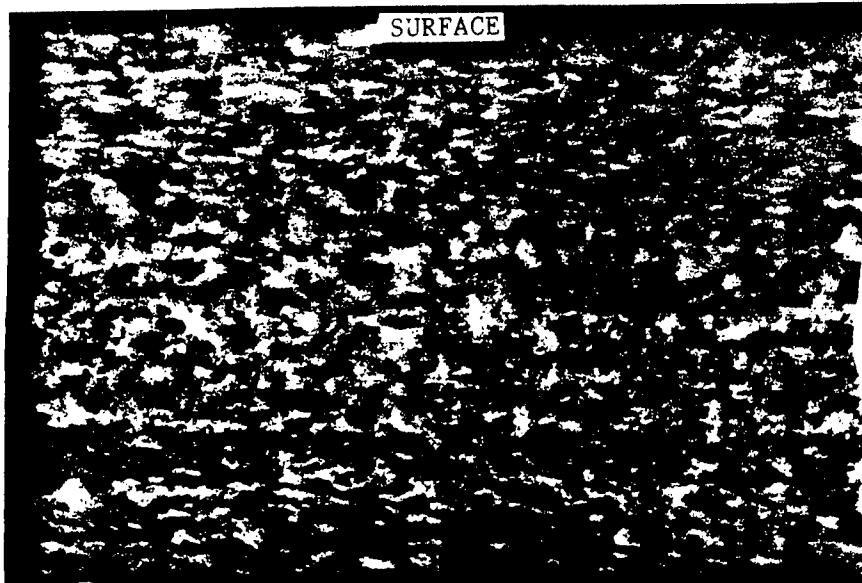


Figure 5-23. A Micrograph of a Recycled Tank Track Pin Showing the Surface Microstructure. Note the Presence of a Spheroidal Network at the Surfaces, and Lack of Slip Bands. $N_f = 38,000$ Cycles. $S_{max} = 194$ ksi. 500X. Fry's Reagent.

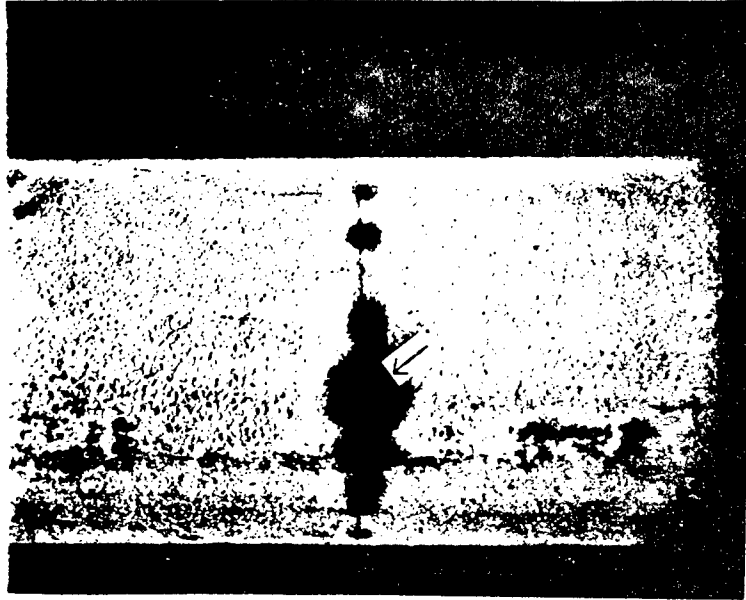


Figure 5-24. A Photo of a Tank Track Pin That Was Fatigued Until a "Ping" Indicated the Presence of a Crack, Showing the Indication Made By Liquid Penitnant Testing.

been shot peened showed that the residual stresses from induction hardening was -15 ksi. The possible fading of residual stresses during the life of a pin was also checked. A significant fading of residual stresses occurred in the pins, as indicated in Table 5-7 from overloading or fatigue stressing above the endurance limit. The residual stresses were reduced from the as received value of -110 to -68 ksi when overloaded, and to -90 ksi when fatigued above the endurance limit. No fading of residual stresses was observed in the pin that was fatigued below the endurance limit.

Another as received pin that was fatigued until a crack had formed, showed a residual stress of -32 ksi at the crack. This indicates the presence of compressive forces which keep the crack closed. The cracked pin used in this testing is one which was stopped after the "ping" occurred and the crack had progressed through the induction hardened zone.

5.3.4.2. Reheat Treated Pins. The residual stress measurement of the surface of reheat treated pins exhibited a residual stress of -90 ksi. This value is 18 percent lower than that measured in as received pins, and occurred even though the peening was conducted to the specified Almen strip intensity. The lower residual stress is attributed to the smaller shot size used in the reprocessing of the pin. Similar results have been reported in tests designed to study the effect of shot size on residual stress¹⁴.

5.3.5. Nondestructive Testing of Pins

The nondestructive testing of fatigued pins experienced some difficulty. Cracks produced by fatiguing the pins could only be detected, when tested after pre-fatigue loading and before reheat treatment, with dye penetrant or Magnaflux in those pins with cracks propagating through the induction hardened case. These pins had been fatigued to the point at which a "ping" indicated the existence of a crack, and the test stopped. Figure 5-24 shows a picture of one of these cracks as indicated by dye penetrant. Similar results occurred when the pins were tested after the reheat treatment. Other pins, also with cracks, avoided detection both before and after re-cycling. These pins failed after only several thousand cycles when fatigue testing was continued. The existence of a microcrack was indicated by a small oxidized region at the origin of the failures. Figure 5-25 exhibits a fractograph of a typical surface from a pin which failed from this microcrack. The depth of this microcrack is 0.004 inch. These cracks avoid detection because the high residual stresses keep the crack tightly closed.

Other investigations are reported to be in progress to study the detection of small fatigue cracks in tank track pins. It is suggested that the best time to observe these microcracks is after the first stage of reheat treatment when the residual stress state is not compressive.

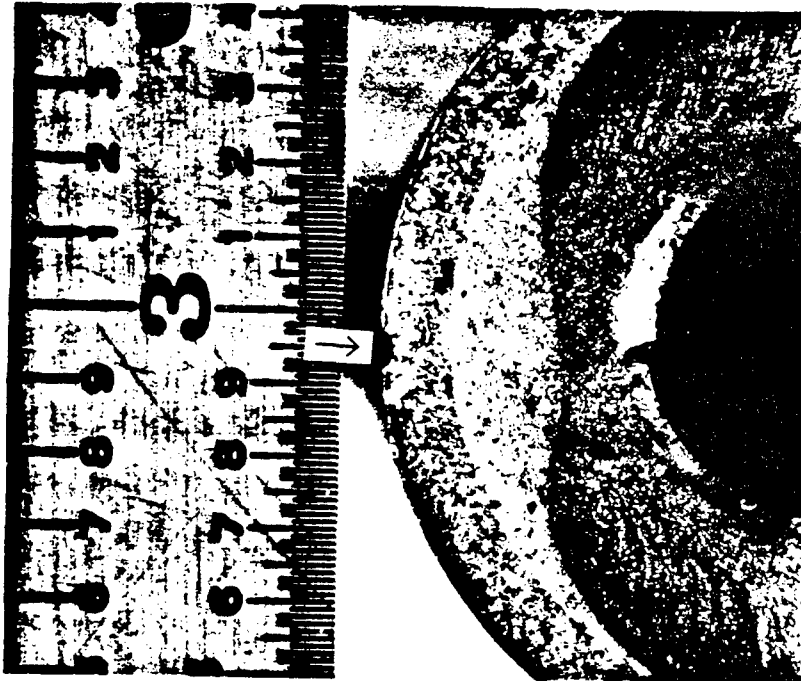


Figure 5-25. A Fractograph of a Recycled Pin That Failed Prematurely, After Reheat Treatment, When Fatigue Testing Was Continued. Note the Presence of a Dark Oxide at the Origin of the Crack (Arrow).

THIS PAGE INTENTIONALLY LEFT BLANK

LIST OF REFERENCES

- 1
"Metals Handbook", 8th edition, Vol. 1, American Society for Metals,
Metals Park, Ohio, 1961.
- 2
Juvinall, R. C., "Stress, Strain and Strength", McGraw-Hill, 1967.
- 3
Dieter, G. E., "Mechanical Metallurgy", McGraw-Hill, 1976.
- 4
Klesnil, M. and Lukas, P., "Fatigue of Metallic Materials", Oxford, 1980.
- 5
McClintok, F. A. and Argon, A. S., "Mechanical Behavior of Materials"
1966.
- 6
Manson, S. S., "Fatigue: A Complex Subject--Some Simple Approximations,"
Experimental Mechanics, Vol. 5, July 1965, pp 193-226.
- 7
Kocanda, S., "Fatigue Failure of Metals", Wydawnictwa Naukowo-Techiczne,
Warsaw, Poland, 1978.
- 8
Grosskreutz, J. C., "Fatigue Mechanisms in the Sub-Creep Range", Metal
Fatigue Damage, ASTM Publication STP 495, 1971, pp 5-60.
- 9
Laird, C., "Mechanisms and Theories of Fatigue", ASM Materials Seminar,
St. Louis, 1979, pp 149-203.
- 10
Shigly, J. E., "Mechanical Engineering Design, McGraw-Hill, 1977.
- 11
Lipson, C. and Juvinal R. C., "Handbook of Stress and Strength",
MacMillan, New York, 1963.
- 12
Breen, D. H. and Wene, E. M. "Fatigue in Machines and Structures-Ground
Vehicles", Fatigue and Microstructure, ASM Materials Seminar, St.
Louis, 1979, pp 57-99.

LIST OF REFERENCES (Continued)

- 13
Fluck, P. G., "The Influence of Surface on the Fatigue Life and Scatter of Test Results of Two Steels," Proc. ASTM, Vol. 51, 1951, pp 584-592.
- 14
Campbell, J. E. "Shot Peening for Improved Fatigue Properties and Stress-Corrosion Resistance, Battelle Laboratories, MCIC Report, Columbus, Ohio, 1971.
- 15
Brookman, J. G. and Kiddel, L., "The Prevention of Fatigue Failure in Metal Parts by Shot Peening", The Failure of Metals by Fatigue, Processing Symposium University of Melbourne Australia, Melbourne University Press, 1946, pp 395-396.
- 16
Weertman J., "Fatigue Crack Propagation Theories," Fatigue and Microstructure, ASM Materials Seminar, St. Louis, 1979, pp 279.
- 17
Frost, N. E., Marsh, K. J. and Pook, L. P., "Metal Fatigue", Clarendon Press, Oxford, 1974.
- 18
Holden, J. "Observations of Cyclic Structures at Large Ranges of Plastic-Strain," Acta Metallurgica, Vol. 11, July 1963.
- 19
Modlen, G. F. and Smith, G. C. "Changes Occurring in the Surface of Mild Steel Specimens During Fatigue Stressing", Journal of Iron and Steel Institute, Vol. 194, 1960, p. 459.
- 20
Helgeland, O., Journal of the Institute of Metals, Vol. 93, 1965, p 570.
- 21
Plumbridge, W. J. and Ryder, D. A. "The Metallography of Fatigue," Metallurgical Review, Vol. 14, 1969, p 136.
- 22
Lloyd, D. J. and Greenough, A. P., "The Effect of Intermediate Annealing on the Fatigue Life of Iron," Metal Science Journal, Vol. 3, 1969, pp 134-139.
- 23
Sinclair, G. M. and Dolan, T. J. "Use of a Recrystallization Method to Study the Nature of Damage in Fatigue of Metals," , Edward Brothers Inc. 1969 pp 134-651. Proceedings of the First U. S. Congress of Metals, Edward Brothers Inc., 1969, pp 134-651.

LIST OF REFERENCES (Continued)

- 24
Wood, W. A., "Formation of Fatigue Cracks," Philosophical Magazine, Vol 3, pp 692-699.
- 25
Young, J. M. and Greenough A. P., "The Effect of Annealing Fatigue Damage in Gold," Journal of the Institute of Metals, Vol. 89, 1960-61.
- 26
Harries, D. R. and Smith, G. C., "Fatigue Damage and Crack Formation in Pure Aluminium," Journal of Metals, Vol. 88, 1959-60, p 182-185.
- 27
MTS Reference Manual, MTS Systems Corporation, Minneapolis.
- 28
Timoshenko, S. P. and Gere, J. M., "Mechanics of Materials", D. Van Nostrand Co., 1972.
- 29
Metals Handbook, 8th edition, Vol. 8, American Society for Metals, Metals Park, Ohio, 1961.
- 30
Samsonov, G. U., "Handbook of Hardness Data" Translated by Ch. Nisenbaum, ed. D. Slutzkin, Keter Press, 1971.
- 31
Johnson, C. A., "Metallographic Principles and Procedures", Leco Corp., 1977.
- 32
Heine, H. J., Ed., Using NDT Effectively, reprint from "Foundry Management & Technology.
- 33
Prevey, P. S., "X-Ray Diffraction Procedures for Residual Stress Measurement", Lambda Research Inc., January 1980.

THIS PAGE LEFT BLANK INTENTIONALLY

DISTRIBUTION LIST

	Copies
Commander US Army Tank-Automotive Command ATTN: DRSTA-RCKT (Mr. Joe Fix) 6300 East 11 Mile Road Warren, MI 48397-5000	10
Commander US Army Tank-Automotive Command ATTN: AMSTA-TSL (Technical Library) Warren, MI 48397-5000	14
Commander Defense Technical Information Center Bldg. 5, Cameron Station ATTN: DDAC Alexandria, VA 22314	12
Commander US Army Tank-Automotive Command ATTN: DRSTA-IRRD 6300 East 11 Mile Road Warren, MI 48397-5000	1
Commander US Army Tank-Automotive Command ATTN: ACO 6300 East 11 Mile Road Warren, MI 48397-5000	1
Commander US Army Tank-Automotive Command ATTN: DRSTA-TSE 6300 East 11 Mile Road Warren, MI 48397-5000	1